

Contents

1	Effective Field Theories: an Introduction	1
1.1	A Historical Example: the Fermi Theory of Weak Interactions	1
1.2	Effective Hamiltonians for Weak Decays	3
1.3	QCD Effects	5
1.3.1	Large Logarithms	6
1.4	Wilsonian Renormalization	8
1.4.1	Renormalization of the Effective Operators	8
1.4.2	Getting Rid of the Renormalization Scale	9
1.5	RG Improved Perturbation Theory	10
1.6	Electroweak Corrections	11
2	$\Delta F = 1$ & $\Delta F = 2$ Effective Hamiltonians and Kaon Decays	13
2.1	Effective Hamiltonian for $\Delta S = 1$ Processes	13
2.1.1	Current-Current Operators	14
2.1.2	Wilson Coefficients and Renormalization	17
2.1.3	QCD Penguin Operators	20
2.1.4	Wilson Coefficients and Renormalization	23
2.1.5	Electroweak Penguin Operators	25
2.1.6	Wilson Coefficients and Renormalization	26
2.1.7	Magnetic Penguin Operators	27
2.1.8	A Note on the Operator Basis	27
2.2	Effective Hamiltonian for $\Delta S = 2$ Processes	29

Chapter 1

Effective Field Theories: an Introduction

The study of effective field theories (EFT) [24] arises from a necessity. In principle, one could evaluate the relevant quantities for some weak processes on the lattice. However, the presence of many different energy scales for any given process makes this approach impractical. What one can do for renormalizable theories is to separate the different contributions coming from the different energy scales and evaluate the high-energy part perturbatively while the low-energy contributions can be evaluated on the lattice. This separation is made possible by EFTs. One such process where EFTs are essential is for the study of non-leptonic decays of light mesons such as pions and kaons.

The fundamental idea behind effective field theories (EFT) started in the opposite manner as we are used to today. We can think of the Fermi theory of Weak interactions as really the first effective theory in the history of the SM. In reality, Fermi developed his theory of Weak interactions [13] in the 1930s, well before we knew that a more general theory was present, the now called SM. The Fermi theory was at the time such a speculative theory that even a prestigious peer-reviewed journal like Nature rejected Fermi's paper. We now know that his theory is in fact a *low energy* equivalent of the SM weak interactions!

In this chapter, we are going to introduce the idea behind EFTs with the pedagogical example of the Fermi theory. Then we're going to make a more rigorous definition through the use of the Operator Product Expansion (OPE) which will divide the problem into two main chunks: the Wilson coefficients which encode all the short distance physics and the effective operators matrix elements which deal with the low energy part of the theory. Moreover, we're going to see that QCD corrections give large-log contributions to the amplitude and how we can deal with these large-logs using the RGEs.

1.1 A Historical Example: the Fermi Theory of Weak Interactions

A first historical example that we need to give to set up the background, which we will later develop in more detail, is the Fermi theory of Weak interactions. This

theory was developed by Fermi in the 30s to explain the phenomena of beta decay. He did this by postulating that the decay process can be described by adding to the free Hamiltonians of the particles in the beta process an interaction term containing the wave functions of the four free particles

$$H_F = H_n^0 + H_p^0 + H_e^0 + H_\nu^0 + \sum_i C_i \int d^3x (\bar{u}_p \hat{O}_i u_n) (\bar{u}_e \hat{O}_i u_\nu). \quad (1.1)$$

Here u_p, u_n, u_e, u_ν denote the wave functions of the four particles.

We now concentrate solely the interaction term which is given by the Hamiltonian density

$$\mathcal{H}_F = \sum_i C_i (\bar{u}_p \hat{O}_i u_n) (\bar{u}_e \hat{O}_i u_\nu). \quad (1.2)$$

A question arises: what are the operators \hat{O}_i ? The answer was found in the deep experimental evidence in the years following the proposed theory.

Firstly, the Hamiltonian needs to be a Lorentz scalar, which implies that the operators need to be one of the fermionic bilinear covariants

$$1 \quad \gamma^\mu \quad \sigma^{\mu\nu} = \frac{i}{2}[\gamma^\mu, \gamma^\nu] \quad \gamma^\mu \gamma_5 \quad \gamma_5. \quad (1.3)$$

In principle, one does not know which combination of bilinears enters the Hamiltonian. In the beginning, Gell-Mann and Feynman thought that, like electromagnetism, the interactions should be vectorial in nature. Moreover, from experimental evidence, it was found that only a single helicity appears: electrons and neutrinos are always left-handed while positrons and anti-neutrino are always right-handed. This is a consequence of parity violation in Weak decays. Therefore, the part of the Hamiltonian containing electrons and neutrino spinors should only contain the part of the wave function with negative helicity. This is found by using the chiral projectors like the ones in equations ???. Through this process, it was found that only the $V - A$ combination gives a meaningful contribution

$$\hat{O}_{V-A} = \frac{1}{2}(\gamma^\mu - \gamma^\mu \gamma_5). \quad (1.4)$$

For neutrinos the chiral form of the operators is exact. For the electron, being massive, they are good if the electron momentum is *high enough*^[1]. According to these considerations, we must replace the spinors by their components with negative chirality. Lorentz invariance requires that even the nucleonic part of the Fermi Hamiltonian has to be $V - A$ type. Extensive experimental analysis has led to the conclusion that the correct form for the nucleonic part is given by

$$\bar{u}_p \gamma^\mu (g_V + g_A \gamma_5) u_n = g_V \bar{u}_p \left(1 - \frac{g_A}{g_V} \gamma_5\right) u_n \quad (1.5)$$

with

$$g_A/g_V = -1.255 \pm 0.006 \quad (1.6)$$

¹This implies that the statement that electrons have only positive helicity is only approximately correct.

This takes into a fact that protons and neutrons are composite particles and that the axial symmetry is broken.

The complete expression for the Hamiltonian interaction term is therefore given by

$$\mathcal{H}_F = -\frac{G_F}{\sqrt{2}}g_V \left[\bar{p}\gamma^\mu \left(1 - \frac{g_A}{g_V}\gamma_5 \right) n \right] [\bar{e}\gamma_\mu(1 - \gamma_5)\nu_e]. \quad (1.7)$$

This result can be exploited to find effective Hamiltonians for all kinds of processes like for the muon decay, in which the Hamiltonian takes the form

$$\mathcal{H}_F = -\frac{G_F}{\sqrt{2}}\bar{\nu}_\mu\gamma^\mu(1 - \gamma_5)\mu\bar{e}^-\gamma_\mu(1 - \gamma_5)\nu_e. \quad (1.8)$$

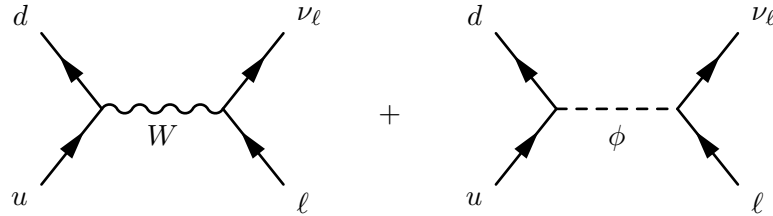
The only problem is now that the theory is clearly non-renormalizable since it is made up of dimension six operators. But fear not, we can circumvent this problem by means of the renormalization group improved perturbation theory which we will explain later.

Here comes the fundamental step: since we know that the SM explains so well weak processes but also does the Fermi theory, the two need to be linked in some way. We will see now that the Fermi theory is a *low energy limit* of the SM.

1.2 Effective Hamiltonians for Weak Decays

We can start by looking at a simpler case of the leptonic decay of a pion $\pi \rightarrow \ell\nu_\ell$, we will see that such a process comes with a much simpler QCD structure due to the presence of quarks only in the initial state.

In the 't Hooft-Feynman gauge² at tree level, this process is governed by two diagrams



The 't Hooft-Feynman is more useful when dealing with loop diagrams since the W propagator does not have the $p^\mu p^\nu$ term like in ?? which would give a complicated ultraviolet behaviour. Moreover, this gauge makes the process of expanding the amplitude more straightforward. The problem is now that we have to deal with Goldstone boson exchange. But since the coupling of the latter is proportional to the light fermion masses, we can ignore them for the following. The amplitude of the W diagram is therefore

$$i\mathcal{A} = \left(\frac{ig_2}{2\sqrt{2}} \right)^2 V_{ud}^* \bar{u}_\ell \gamma^\mu (1 - \gamma_5) \nu_\ell \frac{ig_{\mu\nu}}{s - M_W^2 + i\epsilon} \bar{\nu}_d \gamma^\nu (1 - \gamma_5) u_u. \quad (1.9)$$

²Which is a particular R_ξ gauge with $\xi = 1$.

Given that the typical energy of the process is $s \sim \mathcal{O}(m_\pi) \ll M_W^2$, we can perform an expansion of the W propagator in powers of s , leading to

$$\begin{aligned} i\mathcal{A} &= -i \frac{V_{ud}^* g_2^2}{8M_W^2} \bar{u}_{\nu_\ell} \gamma^\mu (1 - \gamma_5) v_\ell \bar{v}_d \gamma_\mu (1 - \gamma_5) u_u \sum_{k=0}^{\infty} \left(\frac{s}{M_W^2} \right)^k \\ &\simeq -i \frac{G_F}{\sqrt{2}} V_{ud}^* \bar{u}_{\nu_\ell} \gamma^\mu (1 - \gamma_5) v_\ell \bar{v}_d \gamma_\mu (1 - \gamma_5) u_u + \mathcal{O}\left(\frac{s}{M_W^2}\right), \end{aligned} \quad (1.10)$$

where we introduced the Fermi constant as

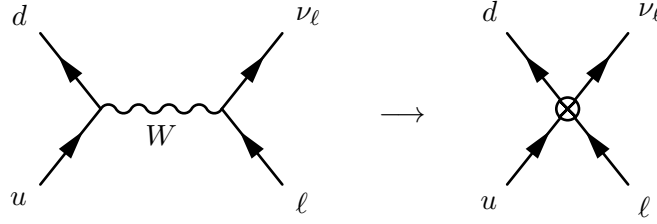
$$\frac{G_F}{\sqrt{2}} = \frac{g_2^2}{8M_W^2}. \quad (1.11)$$

As we can see eq. (1.10) is exactly of the same form as eq. (1.8). This is a first simple example of *operator product expansion* (OPE) [35]: the dominant term in the decay $\pi \rightarrow \ell \nu_\ell$ is given by the matrix element of a six dimensional effective operator

$$Q^{\bar{d}u\bar{\nu}\ell} = \bar{d} \gamma^\mu \frac{(1 - \gamma_5)}{2} u \bar{\nu} \gamma_\mu \frac{(1 - \gamma_5)}{2} \ell \quad (1.12)$$

while subsequent orders $k > 0$ correspond to the matrix elements of higher dimensional operators containing $2k$ derivatives.

From a Feynman diagram point of view, the process of expanding the W propagator, thus making its effects local, amounts to contracting the W propagator to a point



Keeping only dimension six operators in this OPE we obtain that the amplitude is given by

$$\mathcal{A} = \langle \mathcal{H}_{\text{eff}} \rangle + \mathcal{O}\left(\frac{s}{M_W^2}\right) \quad \mathcal{H}_{\text{eff}} = \frac{4G_F}{\sqrt{2}} V_{ud}^* Q^{\bar{d}u\bar{\nu}\ell}, \quad (1.13)$$

where \mathcal{H}_{eff} is the effective Hamiltonian governing the $\pi \rightarrow \ell \nu_\ell$ transition. The process of equating the full amplitude with the one given by the effective Hamiltonian is called *matching*.

The effects of the exchange of the heavy W boson are encoded in the expansion coefficients, which are known as *Wilson coefficients*.

In general, let us consider the amplitude \mathcal{A} of a given process. Thanks to the OPE we can put this in the form

$$\mathcal{A} = \langle \mathcal{H}_{\text{eff}} \rangle = \sum_i C_i(\mu, M_W) \langle Q_i(\mu) \rangle \quad (1.14)$$

when the process takes place at an energy scale $\mu \ll M_W$. We say that the W is being integrated out. The expansion $C_i Q_i$ can be seen as an effective theory

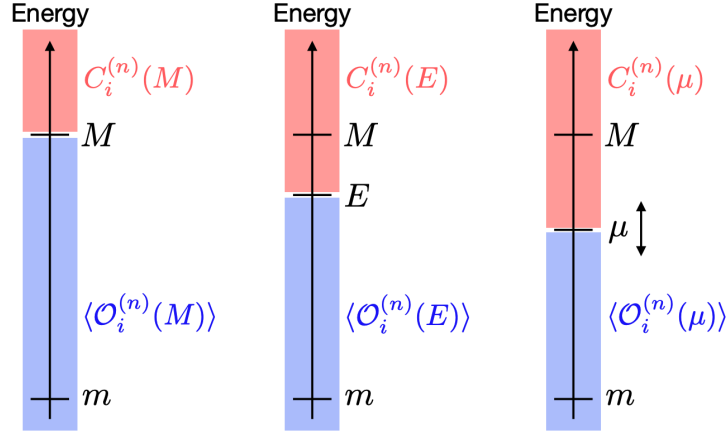


Figure 1.1. Factorization of an observable into short-distance (red) and long-distance (blue) contributions. The panels differ by the choice of the factorization scale. The figure is taken from [26] with the permission of the author.

whose vertices are given by the local operators Q_i and the coupling constants by the expansion coefficients C_i , the Wilson coefficients.

By doing so, we can separate the problem into two main chunks: the Wilson coefficients which contain the short-distance³ contribution to the amplitude and can therefore be evaluated using ordinary perturbation theory and the effective operator matrix elements which contain the low-energy physics and have to be evaluated by means of lattice QCD or other techniques like the large N [31] expansion or chiral perturbation theory (ChPT) [27].

One may roughly think of this process as splitting up the contributions from virtual particles

$$\int_{-p^2}^{M_W^2} \frac{dk^2}{k^2} = \int_{\mu^2}^{M_W^2} \frac{dk^2}{k^2} + \int_{-p^2}^{\mu^2} \frac{dk^2}{k^2}, \quad (1.15)$$

where the first term is sensitive to UV physics and is found into the Wilson coefficients, while the second is sensitive to IR physics and is absorbed into the operator matrix elements. This can be seen pictorially in fig. (1.1).

We note that on a more formal basis, the procedure of the OPE may be given by considering the generating functional for Green functions in the path integral formalism. Then we “integrate out” the heavy degrees of freedom associated with the high scale M from the generating functional of Green’s functions and obtain a non-local action functional, which can be expanded in an infinite tower of local operators $Q_i^{(n)}$ [28].

1.3 QCD Effects

The required QCD corrections to the full theory, in the case of the leptonic decays just mentioned, are the same as the ones in the effective theory since they are just given by external legs corrections and vertex corrections. So under the process of

³High energy.

matching, those won't influence the Wilson coefficients but are going to be contained in the operator matrix element and so we don't need to take them into account.

1.3.1 Large Logarithms

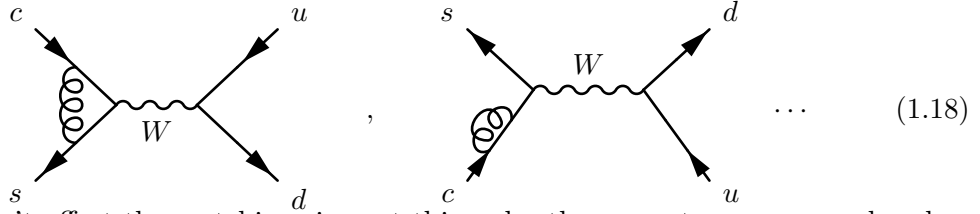
If we now turn to non-leptonic decays, the situation changes drastically. Consider for example the process $c\bar{s} \rightarrow u\bar{d}$. At tree level, after the OPE, we get a dimension six operator which is similar to the one in eq. (1.12)

$$Q_2^{\bar{s}c\bar{d}u} = \bar{s}\gamma^\mu \frac{(1-\gamma_5)}{2} c \bar{u}\gamma_\mu \frac{(1-\gamma_5)}{2} d \equiv \bar{s}_L\gamma^\mu c_L \bar{u}_L\gamma_\mu d_L, \quad (1.16)$$

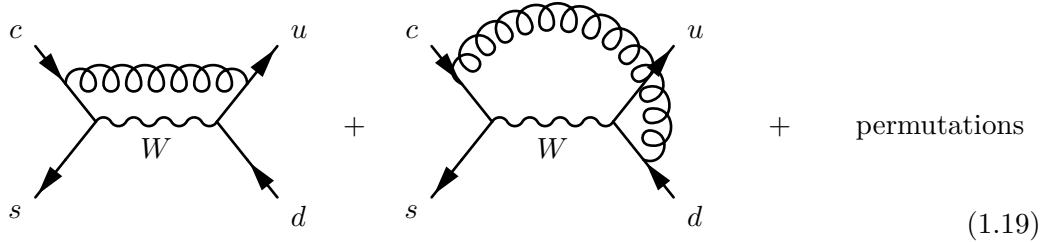
where we used the shorthand notation of the chiral spinors. After matching we get that

$$\mathcal{H}_{\text{eff}} = \frac{4G_F}{\sqrt{2}} V_{cs}^* V_{ud} C_2 Q_2^{\bar{s}c\bar{d}u} \quad C_2 = 1. \quad (1.17)$$

As for the case of the leptonic decay, the Wilson coefficient is trivial at tree level. When we go to $\mathcal{O}(\alpha_s)$ the situation changes drastically. External legs corrections as well as vertex corrections like the ones following



won't affect the matching since at this order the currents are conserved and so they will not generate large-logs. But now, we can have gluon exchange between the initial and the final legs like the following

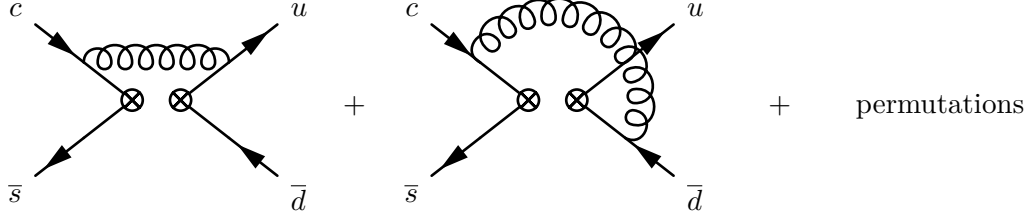


In the full theory this correction will affect the momentum propagating in the W boson, which will make the overall diagram convergent, but proportional to terms of the form

$$\alpha_s \int \frac{d^4\ell}{\ell^2[(p-\ell)^2 - M_W^2]} \sim \alpha_s \log\left(\frac{M_W^2}{-p^2}\right) \quad (1.20)$$

which taken at face value would imply the breakdown of perturbation theory. In fact, when the quark momenta become of the order or Λ_{QCD} , the effective expansion coefficient becomes $\mathcal{O}(1)$. This is the problem of *large logarithms*. Fortunately, the effective theory can save us from this problem.

Let us consider the effective operator for the case at hand $Q_2^{\bar{s}c\bar{d}u}$. The $\mathcal{O}(\alpha_s)$ corrections are given by the following Feynman diagrams



Having removed the W propagator is not a surprise that once we evaluate such diagrams, they come out to be divergent. The effective theory has therefore a much different ultraviolet behaviour with respect to the full SM amplitude. But we know that the EFT is going to be valid up to a cutoff Λ of the order $\mathcal{O}(M_W)$. We can regulate the diagrams by introducing such cutoff, obtaining terms of the form

$$\alpha_s \log \left(\frac{\Lambda^2}{-p^2} \right). \quad (1.21)$$

In reality when dealing with perturbation theory, rather than introducing a specific cutoff, we regulate the theory using dimensional regularization, which introduces a scale μ , and logarithmic terms are going to be of the form $\log(\mu^2 / -p^2)$. When we match the amplitudes of diagrams in eq. (1.19) with the ones in section 1.3.1, any infrared logs cancel and we are left with terms of the form

$$\log \left(\frac{M_W^2}{-p^2} \right) - \log \left(\frac{\mu^2}{-p^2} \right) = \log \left(\frac{M_W^2}{\mu^2} \right). \quad (1.22)$$

We have now the liberty of choosing the matching scale in order to get rid of large logs. In this case, setting $\mu \sim M_W$ we get back the ordinary expansion coefficient α_s , without the log. On the other hand, the non-perturbative part of the hadronic matrix elements needs to be evaluated on the lattice which intrinsically introduces a hard energy cutoff tied to the lattice spacing $a \sim 1/\Lambda$. Then the renormalization of the operators is done, mostly, by the RI-SMOM scheme [25] which is a non-perturbative renormalization scheme suitable to evaluate renormalized quantities on the lattice. Moreover, as we will see in more detail in the following chapter, QCD corrections enlarge the operator basis due to the presence of the gluon which can mix the color of the external quarks, and so a different color structure arises. Not only that but even more complex operators are generated which have the required quantum numbers and therefore have to be taken into account.

Up to here, the point of the situation is as follows: we encounter large logs in the full theory which are a consequence of the many energy scales which enter the process. There is no way to get rid of these large logs. Then, we go to the effective theory where the loop diagrams are divergent and large logs appear with a dependence on the renormalization scale. Through matching, we can get rid of large logs, but only in the Wilson coefficients, which can therefore be evaluated, at a scale $\mu \sim M_W$, with ordinary perturbation theory. The operator matrix elements still contain large logs. We see in the next chapter how the Renormalization Group can help us solve this problem.

1.4 Wilsonian Renormalization

The Wilson coefficients now carry an explicit dependence on the renormalization scale μ which has to cancel out with the renormalization scale dependence of the effective operators, since the full amplitude does not depend on μ

$$0 = \frac{d}{d \log \mu} \mathcal{A} = \frac{dC_i(\mu)}{d \log \mu} \langle Q_i(\mu) \rangle + C_i(\mu) \frac{d\langle Q_i(\mu) \rangle}{d \log \mu}. \quad (1.23)$$

Here $Q_i(\mu)$ are the renormalized composite operators defined in dimensional regularization and the $\overline{\text{MS}}$ scheme, while $C_i(\mu)$ are the corresponding renormalized Wilson coefficients.

What we need to find is the dependence on the renormalization scale of the composite operators.

1.4.1 Renormalization of the Effective Operators

At any order, the basis of effective operators $\{Q_i\}_{i=1,\dots,n}$ can be renormalized in the usual way, as discussed in section ??, by allowing however that the operators can mix under renormalization

$$Q_{i,B} = \sum_{j=1}^n Z_{ij}(\mu) Q_j(\mu). \quad (1.24)$$

Note that the renormalization constants Z_{ij} contain not only the renormalization factors absorbing the UV divergences of the loop corrections to the operator matrix elements, but even a wave-function renormalization factor $Z_q^{1/2}$ for every field contained in the composite operator.

Note that dimensional regularization rules out the possibility of operator mixing between operators of different dimensions. This is one of the reasons why dimensional regularization is the most convenient renormalization scheme in perturbation theory. Given that the bare operators in eq. (1.24) are independent on the renormalization scale, it follows that

$$\frac{dZ_{ij}(\mu)}{d \log \mu} Q_j(\mu) + Z_{ij}(\mu) \frac{dQ_j(\mu)}{d \log \mu} = 0 \quad (1.25)$$

which can be rearranged to give

$$\frac{dQ_i(\mu)}{d \log \mu} = -Z_{ij}^{-1}(\mu) \frac{dZ_{jk}(\mu)}{d \log \mu} Q_k(\mu) \equiv -\gamma_{ik}(\mu) Q_k(\mu), \quad (1.26)$$

where we defined the *anomalous dimension* matrix of the effective operator

$$\gamma(\mu) = \mathbf{Z}^{-1}(\mu) \frac{d\mathbf{Z}(\mu)}{d \log \mu} = \frac{d \log \mathbf{Z}}{d \log \mu}. \quad (1.27)$$

Therefore, the renormalization scale dependence of the effective operator is governed by the Renormalization Group Equation (RGE) in terms of its anomalous dimension

$$\frac{d\vec{Q}(\mu)}{d \log \mu} = -\gamma \cdot \vec{Q}(\mu). \quad (1.28)$$

In analogy with the mass anomalous dimension found in ??, the anomalous dimension matrix of the effective operators can be obtained from the coefficients of the $1/\epsilon$ pole term in Z

$$\gamma = -2\alpha_s \frac{\partial \mathbf{Z}^{(1)}}{\partial \alpha_s}. \quad (1.29)$$

1.4.2 Getting Rid of the Renormalization Scale

Now that the dependence on the renormalization scale of the effective operators is sorted out, we can get back to eq. (1.23). From that, we find that

$$\frac{dC_i(\mu)}{d \log \mu} Q_i(\mu) + C_i(\mu) \frac{dQ_i(\mu)}{d \log \mu} = \left[\frac{dC_i(\mu)}{d \log \mu} \delta_{ij} - C_i(\mu) \gamma_{ij}(\mu) \right] Q_j(\mu) = 0 \quad (1.30)$$

from which follows

$$\frac{d\vec{\mathbf{C}}(\mu)}{d \log \mu} = \gamma^T(\mu) \vec{\mathbf{C}}(\mu). \quad (1.31)$$

This is the differential equation governing the RG evolution of the Wilson Coefficients. In order to solve this equation, we first need to change variable and express the scale dependence of the various quantities via the running QCD coupling $g(\mu)$. Given the definition of the beta function in ??

$$\frac{d}{d \log \mu} = \frac{dg}{d \log \mu} \frac{d}{dg} = \beta(g) \frac{d}{dg} \quad (1.32)$$

then

$$\frac{d\vec{\mathbf{C}}(g(\mu))}{dg} = \frac{\gamma^T(g)}{\beta(g)} \cdot \vec{\mathbf{C}}(g(\mu)). \quad (1.33)$$

This can be solved by means of an integral evolution matrix U defined as

$$\vec{\mathbf{C}}(\mu) = \mathbf{U}(\mu, m) \cdot \vec{\mathbf{C}}(m) \quad (1.34)$$

which can be found iteratively

$$\mathbf{U}(\mu, m) = 1 + \int_{g(m)}^{g(\mu)} dg_1 \frac{\gamma^T(g_1)}{\beta(g_1)} + \int_{g(m)}^{g(\mu)} dg_1 \int_{g(m)}^{g_1} dg_2 \frac{\gamma^T(g_1)}{\beta(g_1)} \frac{\gamma^T(g_2)}{\beta(g_2)} + \dots \quad (1.35)$$

This is exactly the same solution as the Dyson series for the Schrödinger evolution matrix. In fact, eq. (1.33) has the exact same form as Schrödinger's equation, where γ^T/β takes the place of the Hamiltonian. The series expression can be put in a more compact form by introducing the notion of g -ordering

$$\mathbf{U}(\mu, m) = \mathbf{T}_g \exp \left[\int_{g(m)}^{g(\mu)} dg' \frac{\gamma^T(g')}{\beta(g')} \right]. \quad (1.36)$$

1.5 RG Improved Perturbation Theory

With the evolution matrix, we can now run down from the scale $\mu_W \sim M_W$ to a low renormalization scale μ_h closer to the physical scale at which the process we are interested in takes place

$$\vec{\mathcal{C}}(\mu_h) = T_g \exp \left[\int_{g(\mu_h)}^{g(\mu_W)} dg' \frac{\gamma^T(g')}{\beta(g')} \right] \vec{\mathcal{C}}(\mu_W) \quad (1.37)$$

and then compute the relevant matrix elements without encountering large logs since at the scale $\mu_h \sim p_i \sim p_f$ the matrix element

$$\langle f(p_f) | \mathcal{H}_{\text{eff}} | i(p_i) \rangle = C_i(\mu_h) \langle f(p_f) | Q_i | i(p_i) \rangle \quad (1.38)$$

is finite. But where have the large logs gone? They have been resummed by means of the renormalization group! Thus, the effective theory allows us to perform the matching using ordinary perturbation theory and then resum the large logs using the RGE. In general, if we expand the Wilson coefficients and the anomalous dimension matrix in powers of α_s

$$\vec{\mathcal{C}}(\mu) = \sum_{k=0}^n \left(\frac{\alpha_s}{4\pi} \right)^k \vec{\mathcal{C}}^{(k)}(\mu) \quad \gamma = \sum_{k=1}^n \left(\frac{\alpha_s}{4\pi} \right)^k \gamma^{(k)} \quad (1.39)$$

then we can differentiate the perturbative expansion not on the order at which α_s appears, but on the orders resummed by the RGE.

A *leading order* (LO) calculation resums all terms of the form $\mathcal{O}(\alpha_s \log(M_W^2 / -p^2))^n$. In the LO case, we have that

$$\mathcal{A}_{\text{LO}} = C_i^{(0)}(\mu_h) \langle Q(\mu_h)_i \rangle^{(0)}, \quad (1.40)$$

where $\langle Q \rangle^{(n)}$ denotes the matrix element computed at n -th order in strong interaction which are needed to do calculations, and

$$\vec{\mathcal{C}}^{(0)}(\mu_h) = \mathbf{U}^{(0)}(\mu_h, \mu_W) \vec{\mathcal{C}}^{(0)}(\mu_W) \quad \mathbf{U}^{(0)}(\mu_h, \mu_W) = \left(\frac{\alpha_s(\mu_W)}{\alpha_s(\mu_h)} \right)^{\frac{\gamma^{(0)T}}{2\beta_0}}. \quad (1.41)$$

A *(next-to-)^m leading order* (N^mLO) calculation resums all terms of the form $\mathcal{O}(\alpha_s^{n+m} \log^n(M_W^2 / -p^2))$. We now briefly discuss the general result for the NLO case [4]. At NLO we need to evaluate the full and the effective amplitude at $\mathcal{O}(\alpha_s)$

$$\mathcal{A}_{\text{NLO}} = C^{(0)}(\mu_h) \langle Q(\mu_h) \rangle^{(1)} + \frac{\alpha_s(\mu_h)}{4\pi} C^{(1)}(\mu_h) \langle Q(\mu_h) \rangle^{(0)}, \quad (1.42)$$

where again

$$\vec{\mathcal{C}}^{(1)}(\mu_h) = \mathbf{U}(\mu_h, \mu_W) \vec{\mathcal{C}}^{(1)}(\mu_W). \quad (1.43)$$

To this order, the evolution matrix is given by [8]

$$\mathbf{U}^{(1)}(\mu, m) = \left(\mathbb{1} + \frac{\alpha_s(\mu)}{2\pi} \mathbf{J} \right) \mathbf{U}^{(0)}(\mu, m) \left(\mathbb{1} - \frac{\alpha_s(m)}{2\pi} \mathbf{J} \right), \quad (1.44)$$

where $\mathbf{U}^{(0)}$ is the leading order evolution matrix of eq. (1.41). The matrix \mathbf{J} contains the informations about the next-to-leading order corrections. By means of the expansion of the anomalous dimension matrix in eq. (1.39), we define the \mathbf{J} matrix starting from diagonalizing the tree-level anomalous dimension

$$\gamma_D^{(0)} = \mathbf{V}^{-1} \gamma^{(0)T} \mathbf{V}. \quad (1.45)$$

This transformation makes the LO evolution matrix diagonal as well. Then, if we define the following matrix

$$\mathbf{G} = \mathbf{V}^{-1} \gamma^{(1)T} \mathbf{V} \quad (1.46)$$

and another matrix whose elements are

$$H_{ij} = \delta_{ij} \left(\gamma_D^{(0)} \right)_{ij} \frac{\beta_1}{2\beta_0^2} - \frac{G_{ij}}{2\beta_0 + \left(\gamma_D^{(0)} \right)_{ii} - \left(\gamma_D^{(0)} \right)_{jj}} \quad (1.47)$$

the matrix \mathbf{J} is given by

$$\mathbf{J} = \mathbf{V} \mathbf{H} \mathbf{V}^{-1}. \quad (1.48)$$

There is still an important thing to note. From the basic idea of an EFT, whenever we go below some energy threshold, heavy degrees of freedom have to be integrated out. Therefore, what happens when we evolve the Wilson coefficients from the scale of M_W to the scale of m_b , and then we go even below to the scale of m_c and so on? One after the other, quarks become heavy and have to be integrated out. To account for this we need to include a threshold matrix. Following the same principle as in the case of integrating out the W boson, we require that at the scale of the transition μ_t

$$\vec{\mathbf{C}}_f^T(\mu_t) \langle \vec{\mathbf{Q}}_f(\mu_t) \rangle = \vec{\mathbf{C}}_{f-1}^T(\mu_t) \langle \vec{\mathbf{Q}}_{f-1}(\mu_t) \rangle, \quad (1.49)$$

where f is the number of active flavours, which changes from f to $f - 1$ in the transition.

This behaviour can be encompassed in a new evolution matrix which contains a suitable matching matrix \mathbf{T} [11]

$$\mathbf{U}(\mu, M_W) = \mathbf{U}_4(\mu, m_b) \mathbf{T} \mathbf{U}_5(m_b, M_W), \quad (1.50)$$

where $\vec{\mathbf{U}}_f$ is the evolution matrix with f active flavours and

$$\mathbf{T} = \mathbb{1} + \frac{\alpha_s(m_b)}{4\pi} \delta \mathbf{r}^T. \quad (1.51)$$

Equation (1.51) is valid when only strong corrections are present. We will see later the generalization when electroweak corrections are added.

1.6 Electroweak Corrections

We give now a brief summary of the general results that one gets when adding not only strong corrections but electroweak ones. These corrections enter in Penguin-like

operators [33, 34] at leading order. When EM corrections are added, the anomalous dimension matrix at NLO will have the form

$$\gamma = \frac{\alpha_s}{4\pi}\gamma_s^{(0)} + \frac{\alpha_e}{4\pi}\gamma_e^{(0)} + \left(\frac{\alpha_s}{4\pi}\right)^2\gamma_s^{(1)} + \frac{\alpha_e}{4\pi}\frac{\alpha_s}{4\pi}\gamma_{se}^{(1)}, \quad (1.52)$$

where we ignored α_e^2 corrections. Even the evolution matrix will contain corrections of order α_e

$$\mathbf{U}^{(1)}(\mu, m) = \mathbf{M}(\mu)\mathbf{U}^{(0)}(\mu, m)\mathbf{M}'(m), \quad (1.53)$$

where

$$\begin{aligned} \mathbf{M}(\mu) &= \left(\mathbb{1} + \frac{\alpha_e}{4\pi}\mathbf{K}\right)\left(\mathbb{1} + \frac{\alpha_s(\mu)}{4\pi}\mathbf{J}\right)\left(\mathbb{1} + \frac{\alpha_e}{\alpha_s(\mu)}\mathbf{P}\right), \\ \mathbf{M}'(m) &= \left(\mathbb{1} - \frac{\alpha_e}{\alpha_s(m)}\mathbf{P}\right)\left(\mathbb{1} - \frac{\alpha_s(m)}{4\pi}\mathbf{J}\right)\left(\mathbb{1} - \frac{\alpha_e}{4\pi}\mathbf{K}\right), \end{aligned} \quad (1.54)$$

where the running of α_e is not considered. The matrices \mathbf{K}, \mathbf{J} and \mathbf{P} are solutions of the equations [10, 11]

$$\mathbf{P} + \left[\mathbf{P}, \frac{\gamma_s^{(0)T}}{2\beta_0}\right] = \frac{\gamma_e^{(0)T}}{2\beta_0}, \quad (1.55)$$

$$\mathbf{J} - \left[\mathbf{J}, \frac{\gamma_s^{(0)T}}{2\beta_0}\right] = \frac{\beta_1}{2\beta_0^2}\gamma_s^{(0)T} - \frac{\gamma_s^{(1)T}}{2\beta_0}, \quad (1.56)$$

$$\left[\mathbf{K}, \gamma_s^{(0)T}\right] = \gamma_e^{(1)T} + \gamma_e^{(0)T}\mathbf{J} + \gamma_s^{(1)T}\mathbf{P} + \left[\gamma_s^{(0)T}, \mathbf{JP}\right] - 2\beta_1\mathbf{P} - \frac{\beta_1}{\beta_0}\mathbf{P}\gamma_s^{(0)T}. \quad (1.57)$$

Besides the more complicated analytical form of the expressions, the theory stays the same. Once we have the evolution matrix, if we cross a quark mass threshold we need the matching matrix, which in the case of QED+QCD corrections is given by

$$\mathbf{T} = \mathbb{1} + \frac{\alpha_s(\mu)}{4\pi}\delta\mathbf{r}^T + \frac{\alpha_e}{4\pi}\delta\mathbf{s}^T, \quad (1.58)$$

where the nature of the two matrices $\delta\mathbf{r}$ and $\delta\mathbf{s}$ is given by the matching condition at the threshold scale.

Contributions from the Z^0 boson must also be added, but the general form of the solutions given up to now stays the same.

Chapter 2

$\Delta F = 1$ & $\Delta F = 2$ Effective Hamiltonians and Kaon Decays

Using the techniques highlighted in the previous chapter of the OPE and the RGE improved perturbation theory, we are now ready to apply them to the more specific case of $\Delta F = 1$ and $\Delta F = 2$ processes. These two effective theories will describe the non leptonic decays of mesons like K, D, B mesons, and in the case of the $\Delta F = 2$ the oscillation of the neutral mesons such as $K^0 - \bar{K}^0$, $B_d - \bar{B}_d$ and so on.

We will mostly concentrate on the ΔS processes since they are the relevant ones to study the direct and indirect CP-violation in the Kaon system, but the discussion can be easily generalized to different mesons. In particular, we will focus on the following

- The $K \rightarrow 2\pi$ decays, a $\Delta S = 1$ process, where at the quark level the relevant transition is $\bar{s}u \rightarrow \bar{u}d$. This is the process that governs direct CP-violation.
- The $K^0 - \bar{K}^0$ oscillation, a $\Delta S = 2$ process. This is the process that governs indirect CP-violation.

The discussion of the phenomenology of CP-violation in the Kaon system will be given in the subsequent chapter.

2.1 Effective Hamiltonian for $\Delta S = 1$ Processes

As stated in the previous chapter, when we want to analyze low energy processes, due to the appearance of large-logs in the perturbative expansion, we employ the toolkit of effective Hamiltonians.

Consider the process of $K \rightarrow 2\pi$. At tree-level the interactions is mediated by a W -boson exchange with a typical energy of the order $k^2 \sim \mathcal{O}(m_K)$. Therefore, the OPE in this case gives

$$\frac{ig_2^2}{4(k^2 - M_W^2)} V_{us}^* V_{ud} [\bar{v}_s \gamma^\mu (1 - \gamma_5) u_u] [\bar{u}_u \gamma_\mu (1 - \gamma_5) v_d] = -i \frac{G_F}{\sqrt{2}} V_{us}^* V_{ud} Q_2 + \mathcal{O}\left(\frac{k^2}{M_W^2}\right) \quad (2.1)$$

where we find the first effective, current-current, operator

$$Q_2 = \bar{s}_L^i \gamma^\mu u_L^i \bar{u}_L^j \gamma_\mu d_L^j. \quad (2.2)$$

We wrote explicitly how the color indices are summed for reasons that will be obvious in a moment.

After this, we might also need to consider QCD corrections which will enlarge the operator basis. When we do so, we need to evaluate the Feynman diagrams in perturbation theory, both in the full and effective theory as shown, at first order in α_s in fig. (2.1).

One might then think that once these diagrams are taken into account, then there would not be any others. But the reality is that another class of operators needs to be considered, the so-called *penguin operators* [29, 32]. These diagrams play a central role particularly for ϵ'/ϵ and can be mainly divided into three categories: gluonic penguins, electroweak penguins, and magnetic penguins. We will see later in more detail the operators that are generated by such diagrams.

2.1.1 Current-Current Operators

There are two current-current operators. The first one is the operator of eq. (2.2). The fact that is called Q_2 instead of Q_1 is just a convention.

The second current-current operator is generated by the diagrams in fig (2.1), and we will give now the explicit computation. The diagrams we need to consider are just (2.1g) and (2.1h), with their mirror diagrams, since diagram (2.1f), and its mirror, cancel against the renormalization constant of the quark field.

To study the generation of the new operator, we just need to analyze the Dirac structure of the diagram. If we consider all external quark momenta to be zero¹ then the diagram (2.1g) gives in dimensional regularization

$$i\mathcal{A}_g = \frac{4G_F}{\sqrt{2}} V_{us}^* V_{ud} \int \frac{d^d \ell}{(2\pi)^d} \bar{u}_i^u (ig_s \gamma_\mu t_{ij}^a) \frac{i \not{\ell}}{\ell^2} \gamma_\rho P_L v_j^d \bar{v}_k^s \gamma^\rho P_L \frac{i \not{\ell}}{\ell^2} (ig_s \gamma_\nu t_{kl}^b) u_l^u \frac{-ig^{\mu\nu} \delta^{ab}}{\ell^2}, \quad (2.3)$$

where we used the shorthand notation $P_{L/R} = (1 \pm \gamma_5)/2$. Given that $\not{\ell} \Gamma \not{\ell} = \ell^2/d \gamma^\alpha \Gamma \gamma_\alpha$ since there are no other scales involved, we can take out the Dirac structure

$$-i \frac{4G_F}{\sqrt{2}} \frac{g_s^2}{d} \mu^{4-d} t_{ij}^a t_{kl}^a \left(\bar{u}_i^u \gamma_\mu \gamma_\alpha \gamma_\rho P_L v_j^d \right) \left(\bar{v}_k^s \gamma^\rho P_L \gamma^\alpha \gamma^\mu u_l^u \right) \int \frac{d^d \ell}{(2\pi)^d} \frac{1}{\ell^4}. \quad (2.4)$$

We need to manipulate the Dirac structure a bit and to do so we will heavily use the Fierz identities [14, 30] which are just a fancy way of expanding the Dirac algebra on the basis of the matrices $P_L, P_R, \gamma^\nu P_L, \gamma^\nu P_R, \sigma^{\mu\nu}$. In fact, take the following structure

$$P_L v_j^d \bar{v}_k^s \gamma^\rho P_L = P_L v_j^d \bar{v}_k^s P_R \gamma^\rho \implies (P_L v_j^d \bar{v}_k^s P_R)_{\alpha\beta} \quad (2.5)$$

where the equality follows from the Clifford algebra of the γ_5 and we made explicit the Dirac indices. Not considering the γ^ρ , we can project it on the $\gamma^\nu P_R$ element by

¹This will introduce an additional IR divergence which we just ignore since this can be done at the level of accuracy (LO) at which we are working.

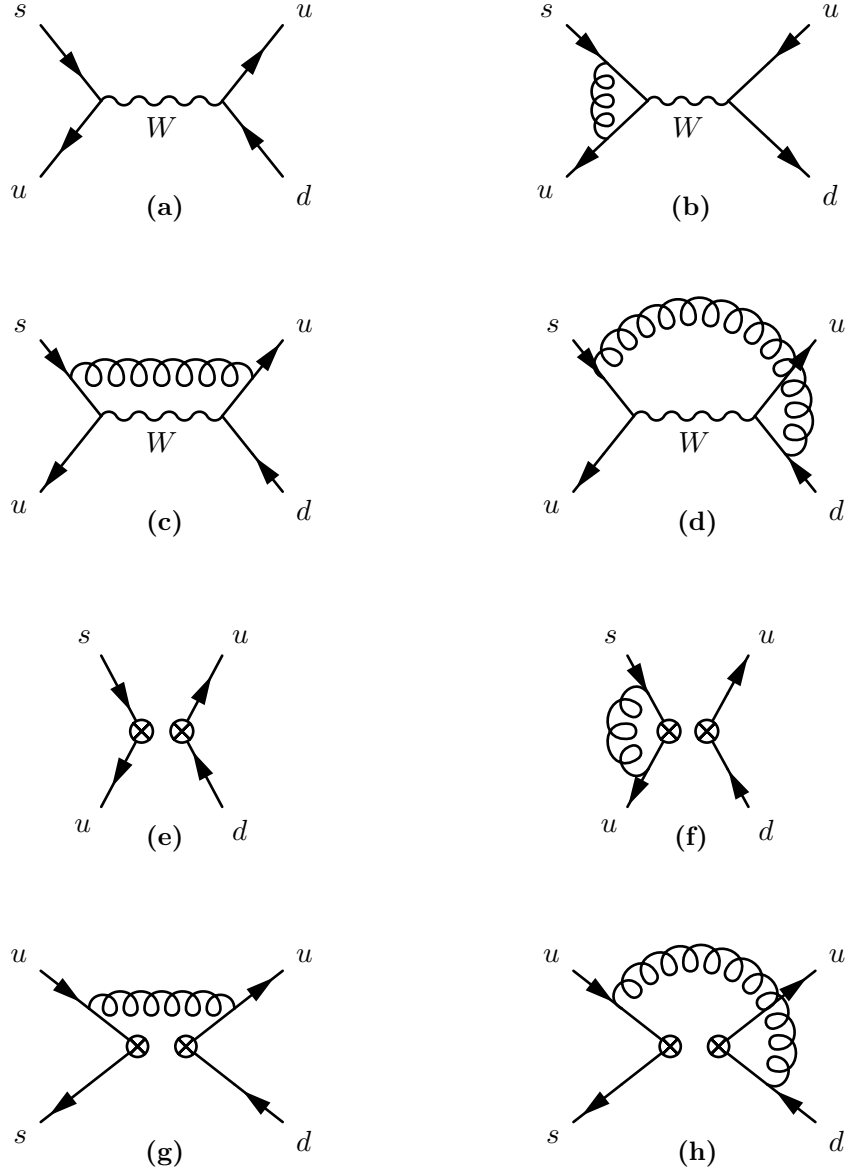


Figure 2.1. Relevant current-current Feynman diagrams for the $s \rightarrow \bar{u} u d$ process in the full and effective theory up to $\mathcal{O}(\alpha_s)$.

using the trace

$$\begin{aligned} \frac{1}{2} \text{Tr} \left(\gamma^\nu P_L P_L v_j^d \bar{v}_k^s P_R \right) &= \frac{1}{2} \text{Tr} \left(\gamma^\nu P_L v_j^d \bar{v}_k^s P_R \right) = \frac{1}{2} \text{Tr} \left(P_R \gamma^\nu P_L v_k \bar{v}_k^s \right) \\ &= -\frac{1}{2} \bar{v}_k^s P_R \gamma^\nu P_L v_j^d, \end{aligned} \quad (2.6)$$

which simply follows from the usual rules for projectors and the anticommuting spinors. Therefore

$$(P_L v_j \bar{v}_k^s P_R)_{\alpha\beta} = -\frac{1}{2} \bar{v}_k^s \gamma^\nu P_L v_j^d (\gamma_\nu P_R)_{\alpha\beta}. \quad (2.7)$$

If we put this in the spinor structure of eq. (2.4) we obtain

$$\begin{aligned} & \left(\bar{u}_i^u \gamma_\mu \gamma_\alpha \gamma_\rho P_L v_j^d \right) \left(\bar{v}_k^s \gamma^\rho P_L \gamma^\alpha \gamma^\mu u_t^u \right) \\ &= -\frac{1}{2} \bar{v}_k^s \gamma^\beta P_L v_j^d \bar{u}_i^u \gamma_\mu \gamma_\alpha \gamma_\rho \gamma^\beta P_R \gamma^\rho \gamma^\alpha \gamma^\mu u_t^u \\ &= -\frac{1}{2} \bar{v}_k^s \gamma^\beta P_L v_j^d \bar{u}_i^u \gamma_\mu \gamma_\alpha \gamma_\rho \gamma^\beta \gamma^\rho \gamma^\alpha \gamma^\mu P_L u_t^u \end{aligned} \quad (2.8)$$

where we can now use the usual rules for the d-dimensional gamma matrices

$$\begin{aligned} \gamma_\mu \gamma_\alpha \underbrace{\gamma_\rho \gamma^\beta \gamma^\rho}_{(2-d)} \gamma^\alpha \gamma^\mu &= (2-d) \gamma_\mu \underbrace{\gamma_\alpha \gamma^\beta \gamma^\alpha}_{(2-d)} \gamma^\mu \\ &= (2-d)^2 \gamma_\alpha \gamma^\beta \gamma^\alpha = (2-d)^3 \gamma^\beta \end{aligned} \quad (2.9)$$

to get

$$\begin{aligned} \left(\bar{u}_i^u \gamma_\mu \gamma_\alpha \gamma_\rho P_L v_j^d \right) \left(\bar{v}_k^s \gamma^\rho P_L \gamma^\alpha \gamma^\mu u_t^u \right) &= -\frac{(2-d)^3}{2} \bar{v}_k^s \gamma^\beta P_L v_j^d \bar{u}_i^u \gamma_\beta P_L u_t^u \\ &= -\frac{(2-d)^3}{2} \bar{v}_k^s \gamma^\beta \left(P_L v_j^d \bar{u}_i^u P_R \right) \gamma_\beta u_t^u. \end{aligned} \quad (2.10)$$

Since the order of the spinors is inverted with respect to Q_2 we can again use the Fierz trick for the bracketed quantity, obtaining

$$\frac{(2-d)^3}{4} \bar{u}_i^u \gamma_\mu P_L v_j^d \bar{v}_k^s \gamma^\beta \gamma^\mu P_R \gamma_\beta u_t^u = \frac{(2-d)^4}{4} \left(\bar{u}_i^u \gamma_\mu P_L v_j^d \right) \left(\bar{v}_k^s \gamma^\mu P_L u_t^u \right) \quad (2.11)$$

henceforth the relevant Dirac structure is back to being

$$\bar{u}_i^u \gamma_\mu P_L v_j^d \bar{v}_k^s \gamma^\mu P_L u_t^u. \quad (2.12)$$

But now comes the important step: the presence of the gluon added an additional $SU(N)$ generator structure that we need to take into account. As we see in eq. (2.4) we have

$$t_{ij}^a t_{kl}^a = \frac{1}{2} \left(\delta_{il} \delta_{jk} - \frac{1}{N} \delta_{ij} \delta_{kl} \right) \quad (2.13)$$

which mixes the color structure of the operator in eq. (2.12) and creates a new operator with the same Dirac structure but mixed color structure

$$\begin{aligned} t_{ij}^a t_{kl}^a \bar{u}_i^u \gamma_\mu P_L v_j^d \bar{v}_k^s \gamma^\mu P_L u_t^u &= \bar{u}_i^u \gamma_\mu P_L v_j^d \bar{v}_k^s \gamma^\mu P_L u_t^u - \frac{1}{N} \bar{u}_i^u \gamma^\mu P_L v_i^d \bar{v}_j^s \gamma_\mu P_L u_j^u \\ &= \langle Q_1 \rangle - \frac{1}{N} \langle Q_2 \rangle. \end{aligned} \quad (2.14)$$

This makes it clear why before we made the color structure of Q_2 evident. The diagram has generated another operator which needs to be considered for the renormalization procedure. Doing a similar calculation for diagram (2.1h) gives the same answer but obviously with a different divergent behaviour due to the loop integral and the different Fierz.

Therefore we have two current-current operators

$$Q_1 = \bar{s}_L^i \gamma^\mu u_L^j \bar{u}_L^j \gamma_\mu d_L^i, \quad Q_2 = \bar{s}_L^i \gamma^\mu u_L^i \bar{u}_L^j \gamma_\mu d_L^j. \quad (2.15)$$

2.1.2 Wilson Coefficients and Renormalization

Before we did not evaluate the integral of diagram (2.1g) since we only needed to control the Dirac structure to find the new effective operator. If we then want to find the Wilson coefficients and the anomalous dimension matrix for the RGE, we need to evaluate the various loop integrals, find the $1/\epsilon$ poles due to the OPE and then match the full and effective theory for the Wilson coefficients.

This is a tremendous task when one takes into account all possible operators since, as we will see later, there are not only current-current ones. Fortunately, the theory for these calculations has been carried out many times before even at NLO including also electromagnetic corrections [4, 8, 11] in the two different regularization schemes NDR and HV. NNLO calculations are also available [6, 17]. Therefore we give here only a summary of the main results with some simple pedagogical calculations.

Where we left off for diagram (2.1g) was, beside the spinors,

$$-i \frac{4G_F}{\sqrt{2}} V_{us}^* V_{ud} g_s^2 \frac{\mu^{4-d}}{8} \frac{(2-d)^4}{d} \int \frac{d^d \ell}{(2\pi)^d} \frac{1}{\ell^4}. \quad (2.16)$$

As we know, the integral vanishes in dimensional regularization, but this is only an artifact of the fact that we chose the external quarks to have zero momentum. Therefore, to solve this integral, as we did in ??, we introduce a fictitious scale and solve the integral with it. After we do so, we set $d = 4 - 2\epsilon$ to get, beside the $4G_F V_{us}^* V_{ud} / \sqrt{2}$ factors,

$$-\frac{i}{8} \left(\frac{4\pi\mu^2}{m^2} \right)^\epsilon \frac{(2\epsilon - 2)^4}{4 - 2\epsilon} \frac{i}{(4\pi)^2} g_s^2 \Gamma(\epsilon), \quad (2.17)$$

which in the limit of $\epsilon \rightarrow 0$

$$\begin{aligned} \left(\frac{4\pi\mu^2}{m^2} \right)^\epsilon &= 1 + \epsilon \log \left(\frac{4\pi\mu^2}{m^2} \right) + \mathcal{O}(\epsilon^2) \\ \Gamma(\epsilon) &= \frac{1}{\epsilon} + \psi(1) + \frac{\epsilon}{2} \left[\frac{\pi^2}{3} + \psi^2(1) - \psi'(1) \right] + \mathcal{O}(\epsilon^2) \\ \frac{(2\epsilon - 2)^4}{4 - 2\epsilon} &= 4 - 14\epsilon + \mathcal{O}(\epsilon^2), \end{aligned} \quad (2.18)$$

eq. (2.17) becomes²

$$\begin{aligned} \frac{\alpha_s}{4\pi} \left[\frac{1}{2\epsilon} - 14 + 4 \log \left(\frac{4\pi\mu^2 e^{-\gamma}}{m^2} \right) \right. \\ \left. + \epsilon \left[(-14 - 4\gamma) \log \left(\frac{4\pi\mu^2}{m^2} \right) + \frac{2\pi^2}{3} - 2\gamma^2 - 2\psi'(1) \right] \right] + \mathcal{O}(\epsilon^2). \end{aligned} \quad (2.19)$$

Retrieving only the $1/\epsilon$ pole we get that the divergent part of the diagram (2.1g) is

$$i\mathcal{A}_g = \frac{4G_F}{\sqrt{2}} V_{us}^* V_{ud} \frac{\alpha_s}{4\pi} \frac{1}{2\epsilon} \left(Q_1 - \frac{1}{3} Q_2 \right), \quad (2.20)$$

where we set $N = 3$.

We can do a similar calculation for diagram (2.1h) that reads

$$i\mathcal{A}_h = \frac{4G_F}{\sqrt{2}} V_{us}^* V_{ud} \int \frac{d^d\ell}{(2\pi)^d} \bar{u}_i^u \gamma_\mu P_L \frac{i\ell}{\ell^2} (ig_s t_{ij}^a \gamma_\beta) v_j^d \bar{v}_k^s \gamma^\mu P_L \frac{i\ell}{\ell^2} (ig_s t_{kl}^b \gamma_\alpha) u_t^u \frac{-ig^{\alpha\beta} \delta^{ab}}{\ell^2}. \quad (2.21)$$

Under the usual simplifications, we get

$$-i \frac{4G_F}{\sqrt{2}} V_{us}^* V_{ud} \frac{g_s^2}{d} \mu^{4-d} t_{ij}^a t_{kl}^a (\bar{u}_i^u \gamma_\mu P_L \gamma_\rho \gamma_\beta v_j^d) (\bar{v}_k^s \gamma^\mu P_L \gamma^\rho \gamma^\beta u_t^u) \int \frac{d^d\ell}{(2\pi)^d}. \quad (2.22)$$

Proceeding on with the Dirac structure simplification, which is a bit more involved in this case when dealing with d-dimensional Clifford algebra, we get

$$\begin{aligned} & \bar{u}_i^u \gamma_\mu \gamma_\rho \gamma_\beta (P_L v_j^d \bar{v}_k^s P_R) \gamma^\mu \gamma^\rho \gamma^\beta u_t^u \\ &= -\frac{1}{2} \bar{v}_k^s \gamma^\alpha P_L v_j^d \bar{u}_i^u \underbrace{\gamma_\mu \gamma_\rho \gamma_\beta \gamma_\alpha \gamma^\mu \gamma^\rho \gamma^\beta}_{\text{Dirac structure}} P_L u_t^u \\ &= \bar{v}_k^s \gamma^\alpha P_L v_j^d \bar{u}_i^u \gamma_\alpha \gamma_\beta \gamma_\rho \gamma^\rho \gamma^\beta P_L u_t^u + \frac{(d-4)}{2} \bar{v}_k^s \gamma^\alpha P_L v_j^d \bar{u}_i^u \gamma_\rho \gamma_\beta \gamma_\alpha \gamma^\rho \gamma^\beta P_L u_t^u. \end{aligned} \quad (2.23)$$

The first bit becomes

$$\begin{aligned} & \bar{v}_k^s \gamma^\alpha P_L v_j^d \bar{u}_i^u \underbrace{\gamma_\alpha \gamma_\beta \gamma_\rho \gamma^\rho \gamma^\beta}_{\text{Dirac structure}} P_L u_t^u \\ &= d^2 \bar{v}_k^s \gamma^\alpha (P_L v_j^d \bar{u}_i^u P_R) \gamma_\alpha u_t^u = -\frac{d^2}{2} \bar{u}_i^u \gamma^\mu P_L v_j^d \bar{v}_k^s \gamma^\alpha \gamma_\mu P_R \gamma_\alpha u_t^u \\ &= -\frac{d^2(2-d)}{2} (\bar{u}_i^u \gamma^\mu P_L v_j^d) (\bar{v}_k^s \gamma_\mu P_L u_t^u), \end{aligned} \quad (2.24)$$

while the second bit

$$\begin{aligned} & \frac{(d-4)}{2} \bar{v}_k^s \gamma^\alpha P_L v_j^d \bar{u}_i^u \underbrace{\gamma_\rho \gamma_\beta \gamma_\alpha \gamma^\rho \gamma^\beta}_{\text{Dirac structure}} P_L u_t^u \\ &= \frac{(d-4)^2}{2} \bar{v}_k^s \gamma^\alpha P_L v_j^d \bar{u}_i^u \gamma_\beta \gamma_\alpha \gamma^\beta P_L u_t^u + 2(d-4) \bar{v}_k^s \gamma^\alpha P_L v_j^d \bar{u}_i^u \gamma_\alpha P_L u_t^u \\ &= -\left[\frac{(d-4)^2(2-d)^2}{4} - (d-4)(2-d) \right] (\bar{u}_i^u \gamma_\mu P_L v_j^d) (\bar{v}_k^s \gamma^\mu P_L u_t^u). \end{aligned} \quad (2.25)$$

²The scale m^2 is not physical. When taking the limit $m^2 \rightarrow 0$ to get back to the original result, we find another divergence which is the IR divergence noted before due to the zero quark momenta.

Therefore the whole expression becomes

$$-\left[\frac{d^2(2-d)}{2} + \frac{(d-4)^2(2-d)^2}{4} - (d-4)(2-d)\right] \left(\bar{u}_i^u \gamma_\mu P_L v_j^d\right) (\bar{v}_k^s \gamma^\mu P_L u_t^u). \quad (2.26)$$

When taking into account the $1/d$ factor from the amplitude in eq. (2.22) and substituting $d = 4 - 2\epsilon$, we obtain

$$\frac{-4(\epsilon-1)^2(\epsilon^2 + \epsilon - 4)}{4 - 2\epsilon} = 16 - 36\epsilon + \mathcal{O}(\epsilon^2). \quad (2.27)$$

Taking only the $1/\epsilon$ pole in eq. (2.22) together with the previous expansion, we find

$$\frac{4G_F}{\sqrt{2}} V_{us}^* V_{ud} \frac{\alpha_s}{4\pi} (-2) \frac{1}{\epsilon} \left(Q_1 - \frac{1}{N} Q_2\right). \quad (2.28)$$

Summing the contribution from diagrams (2.1g) and (2.1h) with their mirrors, we get the final amplitude

$$i\mathcal{A} = \frac{4G_F}{\sqrt{2}} V_{us}^* V_{ud} \frac{\alpha_s}{4\pi} \frac{-3}{\epsilon} \left(Q_1 - \frac{1}{N} Q_2\right) Q_2. \quad (2.29)$$

In order to compute the two-by-two anomalous dimension matrix, we need to compute the one-loop renormalization of the operator Q_1 inserting it in diagrams (2.1g) and (2.1h) and their mirrors. The only difference between this and the ones evaluated before for Q_1 is the color structure given by the $SU(N)$ generators being

$$t_{il}^a t_{kj}^a = \frac{1}{2} \left(\delta_{ij} \delta_{kl} - \frac{1}{N} \delta_{il} \delta_{kj} \right). \quad (2.30)$$

It is clear that this does not generate other operators, therefore if we consider only current-current operators, the discussion ends here. With this, we renormalize the operators as prescribed in eq. (1.24) to obtain, in the $\overline{\text{MS}}$ scheme,

$$\mathbf{Z} = \mathbb{1} + \frac{\alpha_s}{4\pi} \mathbf{Z}_1 = \mathbb{1} + \frac{\alpha_s}{4\pi} \frac{1}{\epsilon} \begin{pmatrix} 3/N & -3 \\ -3 & 3/N \end{pmatrix}, \quad (2.31)$$

which gives the following anomalous dimension matrix, from its definition in eq. (1.27)

$$\gamma^{(0)} = \begin{pmatrix} -6/N & 6 \\ 6 & -6/N \end{pmatrix}. \quad (2.32)$$

In this simple case, the evolution matrix can be found by diagonalizing the anomalous dimension, defining

$$Q_\pm = \frac{Q_1 \pm Q_2}{2}, \quad C_\pm = C_1 \pm C_2, \quad \gamma_\pm^{(0)} = \pm 6 \frac{N \mp 1}{N}, \quad (2.33)$$

therefore

$$U_0^\pm = \left(\frac{\alpha_s(\mu_W)}{\alpha_s(\mu_h)} \right)^{\gamma_\pm^{(0)}/2\beta_0}, \quad (2.34)$$

where $C_{1/2}$ are the Wilson coefficients which, at LO, are just $C_1 = 0$ and $C_2 = 1$. Note that, as we discussed before, β_0 depends on the number of active flavours which means that if we want to evaluate the Wilson coefficients at a scale $\mu_h \sim 2$ GeV we need to take into account the bottom quark threshold at a scale $\mu_b \sim m_b$

$$C_{\pm}(2 \text{ GeV}) = \left(\frac{\alpha_s(\mu_b)}{\alpha_s(2 \text{ GeV})} \right)^{\gamma_{\pm}^{(0)}/2\beta_0(4)} \left(\frac{\alpha_s(\mu_W)}{\alpha_s(2 \text{ GeV})} \right)^{\gamma_{\pm}^{(0)}/2\beta_0}. \quad (2.35)$$

At NLO the situation becomes more complicated. The anomalous dimension matrix needs to be evaluated at $\mathcal{O}(\alpha_s^2)$ and the Wilson coefficients start at

$$C_{\pm}(\mu_W) = 1 \pm \frac{\alpha_s(\mu_W)}{4\pi} 11 \frac{N \mp 1}{2N} \quad (2.36)$$

in the NDR scheme. A complete discussion can be found in [4, 11].

2.1.3 QCD Penguin Operators

Up until now, we found that the effective Hamiltonian for the $\Delta S = 1$ processes, like the decay $K \rightarrow 2\pi$, is built up by two operators

$$\mathcal{H}_{\text{eff}}^{\bar{s} \rightarrow \bar{d}} = \frac{4G_F}{\sqrt{2}} V_{us}^* V_{ud} [C_1 Q_1 + C_2 Q_2]. \quad (2.37)$$

But looking at the quark content of the operators, it is clear that when evaluating their renormalization, additional diagrams arise from the contraction of the u and \bar{u} fields in $Q_{1,2}$ by attaching a gluon, as seen in fig (2.2).

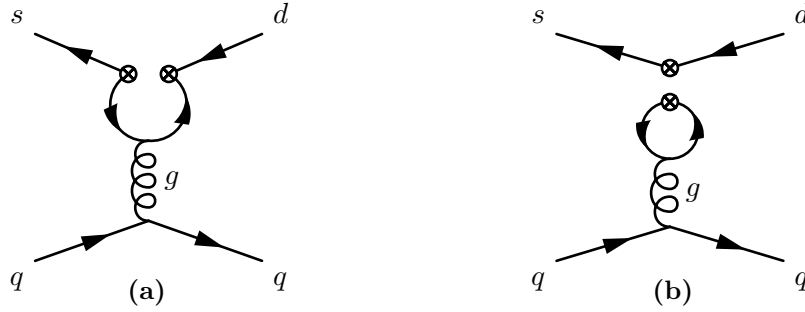


Figure 2.2. Effective QCD Penguins for the $\bar{s} \rightarrow \bar{d}$ transition.

The form of these operators can be easily found by considering that they are FCNC and therefore must be of the form $\bar{s}_i \Gamma^\mu t_{ij}^a d_j$ which cannot be generated at tree-level by the SM Lagrangian. If we take the momenta of the quark to be q , then the possible form of these operators must be

$$\bar{s}_i \Gamma^\mu t_{ij}^a d_j = A(q^2) \bar{s}_i \gamma^\mu t_{ij}^a d_j + B(q^2) \bar{s}_i q^\mu t_{ij}^a d_j + C(q^2) \bar{s}_i \sigma^{\mu\nu} q_\nu t_{ij}^a d_j. \quad (2.38)$$

Given that gauge invariance assures us that $q_\mu \bar{s}_i \Gamma^\mu t_{ij}^a d_j = 0$, we have that

$$A(q^2) \bar{s}_i q^\mu t_{ij}^a d_j + C(q^2) \bar{s}_i q^2 t_{ij}^a d_j = 0 \quad (2.39)$$

by choosing, without loss of generality, $A(q^2) = q^2$ and $B(q^2) = -\not{q}$, we have

$$\bar{s}_i \Gamma^\mu t_{ij}^a d_j = \bar{s}_i (q^2 \gamma^\mu - \not{q} q^\mu) t_{ij}^a d_j + C(q^2) \bar{s}_i \sigma^{\mu\nu} q_\nu t_{ij}^a d_j. \quad (2.40)$$

The second operator connects spinors with different helicity and therefore must be proportional to the quark mass, so for massless quarks cannot be generated.

By using the equations of motion, we see that the first structure corresponds to the matrix elements of the operator $\bar{s}_i \gamma^\mu t_{ij}^a d_j D^\nu G_{\mu\nu}^a$, in fact

$$D^\nu G_{\mu\nu}^a = g_s \sum_f \bar{q}_f^i \gamma_\mu t_{ij}^a q_f^j \quad (2.41)$$

where f is any active quark flavour, gives

$$\bar{s}_i \gamma_\mu t_{ij}^a d_j \sum_f \bar{q}_f^k \gamma^\mu t_{kl}^a q_f^l. \quad (2.42)$$

Consider diagram (2.2a) with the insertion of the operator of eq. (2.40), roughly speaking

$$\bar{q}_f \gamma^\mu t^a q_f \frac{1}{q^2} \bar{s} (q^2 \gamma_\mu - q_\mu \not{q}) t^a d \quad (2.43)$$

since the quarks q_f carry momentum q , due to the equation of motion $q_\mu q_f = 0$, therefore there remain just

$$\bar{q}_f \gamma^\mu t^a q_f \frac{1}{q^2} \bar{s} q^2 \gamma_\mu t^a d, \quad (2.44)$$

where the q^2 cancels with the pole of the propagator, leaving just the matrix element of the local operator in eq. (2.42)

$$\bar{s} \gamma^\mu t^a d \bar{q}_f \gamma_\mu t^a q. \quad (2.45)$$

These diagrams are log-divergent which means that they need to be renormalized forcing us to enlarge the operator basis again. When inserting operators $Q_{1/2}$ in the effective vertex of the gluonic penguin a total of four more operators is generated

$$\begin{aligned} Q_3 &= \bar{s}_L^i \gamma^\mu d_L^i \sum_f \bar{q}_{fL}^j \gamma_\mu q_{fL}^j, \\ Q_4 &= \bar{s}_L^i \gamma^\mu d_L^j \sum_f \bar{q}_{fL}^j \gamma_\mu q_{fL}^i, \\ Q_5 &= \bar{s}_L^i \gamma^\mu d_L^i \sum_f \bar{q}_{fR}^j \gamma_\mu q_{fR}^j, \\ Q_6 &= \bar{s}_L^i \gamma^\mu d_L^j \sum_f \bar{q}_{fR}^j \gamma_\mu q_{fR}^i. \end{aligned} \quad (2.46)$$

As a matter of fact, we give a little computation to see how these operators are generated by considering the diagram (2.2a) with the insertion of operator Q_2 in

the effective vertex. Again we consider the external quark momenta to be zero and the momentum flowing in the gluon to be q .

$$\begin{aligned} i\mathcal{A} &= \int \frac{d^d\ell}{(2\pi)^d} \bar{v}_i^d \gamma^\mu P_L \frac{i(\ell - \not{q})}{(\ell - q)^2} (ig_s t_{ij}^a \gamma^\alpha) \frac{i\ell}{\ell^2} \gamma_\mu P_L v_j^s \bar{u}_k^q (ig_s t_{kl}^b \gamma^\beta) u_l^q \frac{-ig_{\alpha\beta} \delta^{ab}}{q^2} \\ &= -i\mu^{4-d} \frac{g_s^2}{q^2} \left(\bar{v}_i^d \gamma^\mu P_L \gamma^\rho t_{ij}^a \gamma^\alpha \gamma^\sigma \gamma_\mu P_L v_j^s \right) (\bar{u}_k^q \gamma_\alpha t_{kl}^a u_l^q) I_{\rho\sigma}, \end{aligned} \quad (2.47)$$

where the integral, without going into much details, is just

$$I_{\rho\sigma} = -\frac{i}{16\pi^2} \left(\frac{g_{\rho\sigma}}{2} q^2 + q_\rho q_\sigma \right) \frac{1}{6\epsilon} + \mathcal{O}(\epsilon^0). \quad (2.48)$$

Putting this into the amplitude, we find, besides constant factors³

$$\begin{aligned} & \left(\bar{v}_i^d \gamma^\mu P_L \gamma^\rho t_{ij}^a \gamma^\alpha \gamma^\sigma \gamma_\mu P_L v_j^s \right) (\bar{u}_k^q \gamma_\alpha t_{kl}^a u_l^q) \left(\frac{g_{\rho\sigma}}{2} + q_\rho q_\sigma \right) \frac{1}{q^2} \\ &= \frac{1}{2} \bar{v}_i^d t_{ij}^a \gamma^\mu P_L \left(\gamma^\rho \gamma^\alpha \gamma_\rho + 2 \frac{\not{q} \gamma^\alpha \not{q}}{q^2} \right) \gamma_\mu P_L v_j^s \bar{u}_k^q \gamma_\alpha t_{kl}^a u_l^q. \end{aligned} \quad (2.49)$$

Given that $\gamma^\rho \gamma^\alpha \gamma_\rho = -2\gamma^\alpha$ and that $\gamma^\alpha \not{q} = \{\gamma^\alpha, \not{q}\} - \not{q} \gamma^\alpha = 2q^\alpha - \not{q} \gamma^\alpha$, the parenthesis becomes

$$\left(\gamma^\rho \gamma^\alpha \gamma_\rho + 2 \frac{\not{q} \gamma^\alpha \not{q}}{q^2} \right) = -4 \left(\gamma^\alpha - \frac{\not{q} q^\alpha}{q^2} \right) \quad (2.50)$$

and therefore the Dirac structure is

$$q^2 \bar{v}_i^d t_{ij}^a \gamma^\mu P_L (q^2 \gamma^\alpha - q^\alpha \not{q}) \gamma_\mu P_L v_j^s \bar{u}_k^q \gamma_\alpha t_{kl}^a u_l^q. \quad (2.51)$$

which gives back the FCNC vertex we conjectured earlier.

It is clear now that in the quark loop of the penguin diagram there can also run the charm quark, but not the top quark since it has been integrated out by the OPE. In the full theory even the top quark is present, but not in the low energy one. This means that we should add to the effective Hamiltonian for the $\bar{s} \rightarrow \bar{d}$ transition even the current-current operators with the charm quark, leading to

$$\mathcal{H}_{\text{eff}}^{\bar{s} \rightarrow \bar{d}} = \frac{4G_F}{\sqrt{2}} \left[V_{us}^* V_{ud} (C_1 Q_1^{\bar{s}u\bar{u}d} + C_2 Q_2^{\bar{s}u\bar{u}d}) + V_{cs}^* V_{cd} (C_1 Q_1^{\bar{s}c\bar{c}d} + C_2 Q_2^{\bar{s}c\bar{c}d}) \right]. \quad (2.52)$$

When these operators are inserted into the penguin diagrams, they will give exactly the same divergent part since it does not depend on the mass of the quarks. Therefore the penguin diagram is going to be generated with a coefficient

$$V_{us}^* V_{ud} + V_{cs}^* V_{cd} = -V_{ts}^* V_{td} \quad (2.53)$$

³For simplicity we go back to $d = 4$ since we just want to understand the Dirac structure.

due to the unitarity relation of the CKM matrix. All in all, the full effective Hamiltonian including current-current operators and QCD penguins becomes

$$\mathcal{H}_{\text{eff}}^{\bar{s} \rightarrow \bar{d}} = \frac{4G_F}{\sqrt{2}} \left\{ V_{us}^* V_{ud} \left[C_1 (Q_1^{\bar{s}u\bar{u}d} - Q_1^{\bar{s}c\bar{c}d}) + C_2 (Q_2^{\bar{s}u\bar{u}d} - Q_2^{\bar{s}c\bar{c}d}) \right] - V_{ts}^* V_{td} \left[Q_1^{\bar{s}c\bar{c}d} + C_2 Q_2^{\bar{s}c\bar{c}d} + \sum_{i=1}^6 C_i Q_i^{\bar{s}d} \right] \right\}, \quad (2.54)$$

where again the CKM unitarity has been used to eliminate the factor $V_{cs}^* V_{cd}$.

2.1.4 Wilson Coefficients and Renormalization

Since we have now a total of six operators, the RGE is governed by a 6×6 anomalous dimension matrix which has to be evaluated by inserting all the current-current as well as QCD penguin operators in diagrams (2.1e) to (2.1h) and in the penguin diagrams (2.2a) and (2.2b).

To perform the matching for the Wilson coefficients, one needs also to evaluate the full theory equivalent of the penguin diagram in fig. (2.3) where now even the top quark can run in the loop.

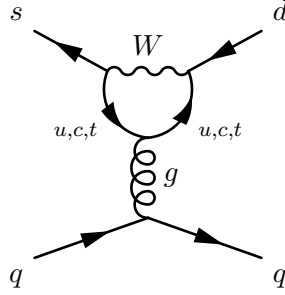


Figure 2.3. QCD penguin in the full theory.

At LO the anomalous dimension matrix $\gamma^{(0)}$ has the explicit form [2, 15, 16, 18, 32]

$$\gamma^{(0)} = \begin{pmatrix} \frac{-6}{N} & 6 & 0 & 0 & 0 & 0 \\ 6 & \frac{-6}{N} & \frac{-2}{3N} & \frac{2}{3} & \frac{-2}{3N} & \frac{2}{3} \\ 0 & 0 & \frac{-22}{3N} & \frac{22}{3} & \frac{-4}{3N} & \frac{3}{4} \\ 0 & 0 & 6 - \frac{2f}{3N} & \frac{-6}{N} + \frac{2f}{3} & \frac{-2f}{3N} & \frac{2f}{3} \\ 0 & 0 & 0 & 0 & \frac{6}{N} & -6 \\ 0 & 0 & \frac{-2f}{3N} & \frac{2f}{3} & \frac{-2f}{3N} & \frac{-6(-1+N^2)}{N} + \frac{2f}{3} \end{pmatrix}, \quad (2.55)$$

while at NLO the second order expansion coefficient of the anomalous dimension

matrix reads [8, 11]

$$\gamma^{(1)} \Big|_{N=3} = \begin{pmatrix} -\frac{21}{2} - \frac{2f}{9} & \frac{7}{2} + \frac{2f}{3} & \frac{79}{9} & -\frac{7}{3} & -\frac{65}{9} & -\frac{7}{3} \\ \frac{7}{2} + \frac{2f}{3} & -\frac{21}{2} - \frac{2f}{9} & -\frac{202}{243} & \frac{1354}{81} & -\frac{1192}{243} & \frac{904}{81} \\ 0 & 0 & -\frac{5911}{486} + \frac{71f}{9} & \frac{5983}{162} + \frac{f}{3} & -\frac{2384}{243} - \frac{71f}{9} & \frac{1808}{81} - \frac{f}{3} \\ 0 & 0 & \frac{379}{18} + \frac{56f}{243} & -\frac{91}{6} + \frac{808f}{81} & -\frac{130}{243} - \frac{502f}{243} & -\frac{14}{3} + \frac{646f}{81} \\ 0 & 0 & -\frac{61f}{9} & -\frac{11f}{3} & \frac{71}{3} + \frac{61f}{9} & -99 + \frac{11f}{3} \\ 0 & 0 & -\frac{682f}{243} & \frac{106f}{81} & -\frac{225}{2} + \frac{1676f}{243} & -\frac{1343}{6} + \frac{1348f}{81} \end{pmatrix}, \quad (2.56)$$

where f is the number of active quark flavours at the scale μ . Both matrices are given in the NDR scheme; the HV scheme results can be found in the sources just cited.

The fact that the top quark can run in the penguin loop in the full theory is fundamental since when performing the matching, one finds that the top quark contribution generates a non-trivial contribution to the $C_{3-6}(\mu_W)$ Wilson coefficients, while the contributions from u and c quarks cancels up to a constant and corrections of order p^2/M_W^2 [8, 22]. After matching, one finds the following Wilson coefficients at NLO

$$\begin{aligned} C_1(M_W) &= \frac{11}{2} \frac{\alpha_s(M_W)}{4\pi}, \\ C_2(M_W) &= 1 - \frac{11}{6} \frac{\alpha_s(M_W)}{4\pi}, \\ C_3(M_W) &= -\frac{\alpha_s(M_W)}{24\pi} \tilde{E}_0(x_t), \\ C_4(M_W) &= \frac{\alpha_s(M_W)}{8\pi} \tilde{E}_0(x_t), \\ C_5(M_W) &= -\frac{\alpha_s(M_W)}{24\pi} \tilde{E}_0(x_t), \\ C_6(M_W) &= \frac{\alpha_s(M_W)}{8\pi} \tilde{E}_0(x_t), \end{aligned} \quad (2.57)$$

where

$$\begin{aligned} E_0(x) &= -\frac{2}{3} \log x + \frac{x(18 - 11x - x^2)}{12(1 - x)^3} + \frac{x^2(15 - 16x + 4x^2)}{6(1 - x)^4} \log x, \\ \tilde{E}_0(x) &= E_0(x) - \frac{2}{3} \end{aligned} \quad (2.58)$$

with $x_t = m_t^2/M_W^2$. It is easy to see that coefficients C_{3-6} are directly related to the top quark as stated before.

2.1.5 Electroweak Penguin Operators

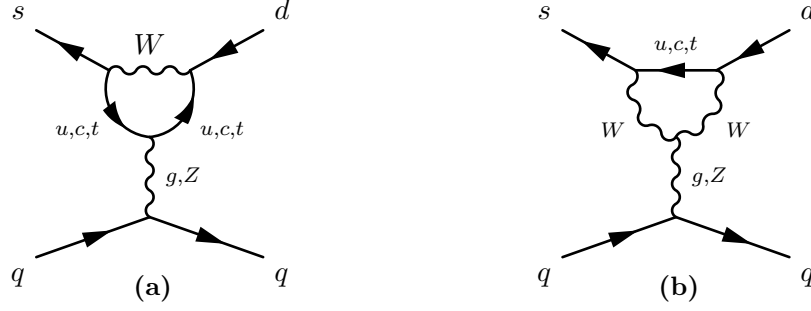


Figure 2.4. Electroweak penguin diagrams for the $\bar{s} \rightarrow \bar{d}$ process.

One may now ask the question of what would happen if the gluons in the QCD penguin diagrams of figs. (2.2) and (2.3) were to be replaced by a photon exchange. Then, electromagnetic corrections will also get log-enhanced making them comparable with the NLO-QCD corrections $\alpha \log(\mu_W^2/\mu_h^2) \sim \alpha_s$. These contributions do not need to be resummed but should be included when working with NLO-QCD [7, 11]. The relevant diagrams that we need to consider when dealing with EW contributions are given in fig. (2.4a).

When introducing also EW contributions, the operator basis needs to be enlarged again. While FCNC of diagram (2.4a) is equivalent to the gluonic one, the equation of motion introduces an explicit charge dependence giving rise to the operator structures

$$\begin{aligned}
 Q_7 &= \frac{3}{2} \bar{s}_L^i \gamma^\mu d_L^i \sum_f e_q \bar{q}_{fL}^j \gamma_\mu q_{fL}^j, \\
 Q_8 &= \frac{3}{2} \bar{s}_L^i \gamma^\mu d_L^j \sum_f e_q \bar{q}_{fL}^j \gamma_\mu q_{fL}^i, \\
 Q_9 &= \frac{3}{2} \bar{s}_L^i \gamma^\mu d_L^i \sum_f e_q \bar{q}_{fR}^j \gamma_\mu q_{fR}^j, \\
 Q_{10} &= \frac{3}{2} \bar{s}_L^i \gamma^\mu d_L^j \sum_f e_q \bar{q}_{fR}^j \gamma_\mu q_{fR}^i.
 \end{aligned} \tag{2.59}$$

When performing the matching for the new EW-penguin operators, as in the case for the gluonic one, one gets a contribution also from the top quark running in the loop. But in this case, this is not the only contribution. One must also consider the diagram where a Z^0 boson is exchanged and the box diagrams (2.6) where two W bosons are exchanged so that one can obtain a gauge-invariant result.

2.1.6 Wilson Coefficients and Renormalization

The RGE is now governed by a 10×10 anomalous dimension matrix, whose LO form is given by

$$\gamma_s^{(0)} = \begin{pmatrix} -\frac{6}{N_c} & 6 & -\frac{2}{3N_c} & \frac{2}{3} & -\frac{2}{3N_c} & \frac{2}{3} & 0 & 0 & 0 & 0 \\ 6 & -\frac{6}{N_c} & 0 & 0 & 0 & 0 & 0 & 0 & 0 & 0 \\ 0 & 0 & -\frac{22}{3N_c} & \frac{22}{3} & -\frac{4}{3N_c} & \frac{4}{3} & 0 & 0 & 0 & 0 \\ 0 & 0 & 6 - \frac{2n_f}{3N_c} & -\frac{6}{N_c} + \frac{2n_f}{3} & -\frac{2n_f}{3N_c} & \frac{2n_f}{3} & 0 & 0 & 0 & 0 \\ 0 & 0 & 0 & 0 & \frac{6}{N_c} & -6 & 0 & 0 & 0 & 0 \\ 0 & 0 & -\frac{2n_f}{3N_c} & \frac{2n_f}{3} & -\frac{2n_f}{3N_c} & 6\frac{1-N_c^2}{N_c} + \frac{2n_f}{3} & 0 & 0 & 0 & 0 \\ 0 & 0 & 0 & 0 & 0 & 0 & \frac{6}{N_c} & -6 & 0 & 0 \\ 0 & 0 & -\frac{2(n_u-n_d/2)}{3N_c} & \frac{2(n_u-n_d/2)}{3} & -\frac{2(n_u-n_d/2)}{3N_c} & \frac{2(n_u-n_d/2)}{3} & 0 & 6\frac{1-N_c^2}{N_c} & 0 & 0 \\ 0 & 0 & \frac{2}{3N_c} & -\frac{2}{3} & \frac{2}{3N_c} & -\frac{2}{3} & 0 & 0 & -\frac{6}{N_c} & 6 \\ 0 & 0 & -\frac{2(n_u-n_d/2)}{3N_c} & \frac{2(n_u-n_d/2)}{3} & -\frac{2(n_u-n_d/2)}{3N_c} & \frac{2(n_u-n_d/2)}{3} & 0 & 0 & 6 & -\frac{6}{N_c} \end{pmatrix}, \quad (2.60)$$

where n_d is the number of active down-like quarks and n_u the one of up-like quarks. Moreover $n_f = n_u + n_d$. The NLO anomalous dimension will have contributions from $\mathcal{O}(\alpha_s^2)$ corrections, but also $\mathcal{O}(\alpha)$ and $\mathcal{O}(\alpha_s \alpha)$, like in eq. (1.52). The specific form of the other coefficients can be found in [7, 11].

The NLO Wilson coefficients at the high scale are found by the matching procedure to be

$$\begin{aligned} C_1(M_W) &= \frac{11}{2} \frac{\alpha_s(M_W)}{4\pi} \\ C_2(M_W) &= 1 - \frac{11}{6} \frac{\alpha_s(M_W)}{4\pi} - \frac{35}{18} \frac{\alpha}{4\pi}, \\ C_3(M_W) &= -\frac{\alpha_s(M_W)}{24\pi} \tilde{E}_0(x_t) + \frac{\alpha}{6\pi \sin^2 \theta_W} [2B_0(x_t) + C_0(x_t)] \\ C_4(M_W) &= \frac{\alpha_s(M_W)}{8\pi} \tilde{E}_0(x_t), \\ C_5(M_W) &= -\frac{\alpha_s(M_W)}{24\pi} \tilde{E}_0(x_t), \\ C_6(M_W) &= \frac{\alpha_s(M_W)}{8\pi} \tilde{E}_0(x_t), \\ C_7(M_W) &= \frac{\alpha}{6\pi} [4C_0(x_t) + \tilde{D}_0(x_t)], \\ C_8(M_W) &= 0, \\ C_9(M_W) &= \frac{\alpha}{6\pi} \left[4C_0(x_t) + \tilde{D}_0(x_t) + \frac{1}{\sin^2 \theta_W} (10B_0(x_t) - 4C_0(x_t)) \right] \\ C_{10}(M_W) &= 0, \end{aligned} \quad (2.61)$$

where

$$\begin{aligned}
B_0(x) &= \frac{1}{4} \left[\frac{x}{1-x} + \frac{x \ln x}{(x-1)^2} \right] \\
C_0(x) &= \frac{x}{8} \left[\frac{x-6}{x-1} + \frac{3x+2}{(x-1)^2} \ln x \right] \\
D_0(x) &= -\frac{4}{9} \ln x + \frac{-19x^3 + 25x^2}{36(x-1)^3} + \frac{x^2(5x^2 - 2x - 6)}{18(x-1)^4} \ln x \\
\tilde{D}_0(x_t) &= D_0(x_t) - \frac{4}{9}.
\end{aligned} \tag{2.62}$$

2.1.7 Magnetic Penguin Operators

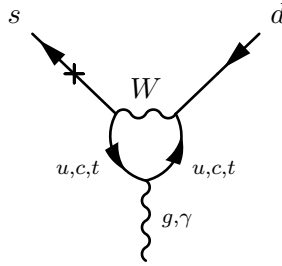


Figure 2.5. Magnetic penguin operators.

In principle, two additional operators contribute to the $\Delta S = 1$ transitions. These are known as *chromomagnetic* and *electromagnetic* penguin operators and have the following form

$$Q_{11} = \frac{g_s}{16\pi^2} m_s \bar{s}_i \sigma^{\mu\nu} t_{ij}^a G_{\mu\nu}^a (1 - \gamma_5) d_j, \quad Q_{12} = \frac{ee_d}{16\pi^2} m_s \bar{s} \sigma^{\mu\nu} F_{\mu\nu} (1 - \gamma_5) d. \tag{2.63}$$

However their contribution for the $K \rightarrow 2\pi$ transitions are chiral suppressed two times: one from the strange mass term and one from the operator matrix element [3, 12], therefore we will not consider them from now on. Even in the RBC lattice analysis, [1] this operator was excluded.

2.1.8 A Note on the Operator Basis

What we found until now is that the $|\Delta S| = 1$ transitions can be described by an effective Hamiltonian containing ten operators

- **Current-Current Operators:**

$$Q_1 = (\bar{s}_i \gamma^\mu P_L u_j)(\bar{u}_j \gamma_\mu P_L d_i) \quad Q_2 = (\bar{s}_i \gamma^\mu P_L u)(\bar{u}_j \gamma_\mu P_L d) \tag{2.64}$$

- **QCD-Penguins Operators**

$$\begin{aligned}
Q_3 &= (\bar{s}_i \gamma^\mu P_L d) \sum_q (\bar{q}_j \gamma_\mu P_L q) & Q_4 &= (\bar{s}_i \gamma^\mu P_L d_j) \sum_q (\bar{q}_j \gamma_\mu P_L q_i) \\
Q_5 &= (\bar{s}_i \gamma^\mu P_L d) \sum_q (\bar{q}_j \gamma_\mu P_R q) & Q_6 &= (\bar{s}_i \gamma^\mu d_j) \sum_q (\bar{q}_j \gamma_\mu P_R q_i)
\end{aligned} \tag{2.65}$$

- **Electrowark-Penguins Operators**

$$\begin{aligned}
Q_7 &= \frac{3}{2}(\bar{s}\gamma^\mu P_L d) \sum_q e_q(\bar{q}\gamma_\mu P_R q) & Q_8 &= \frac{3}{2}(\bar{s}_i\gamma^\mu P_L d_j) \sum_q e_q(\bar{q}_j\gamma_\mu P_R q_i) \\
Q_9 &= \frac{3}{2}(\bar{s}\gamma^\mu P_L d) \sum_q e_q(\bar{q}\gamma_\mu P_L q) & Q_{10} &= \frac{3}{2}(\bar{s}_i\gamma^\mu P_L d_j) \sum_q e_q(\bar{q}_j\gamma_\mu P_L q_i)
\end{aligned} \tag{2.66}$$

where $P_{L/R} = (1 \mp \gamma_5)/2$ are the chiral projectors and e_q is the quark charge in units of e .

These operators are useful in the lattice calculations but when it comes to renormalization, another basis is better suited for the task: the so-called *chiral basis*. This comes in handy since in the usual 10-operator basis, the operators are not linearly independent. In fact, by Fierz transforming operators Q_1 , Q_2 and Q_3

$$\begin{aligned}
\tilde{Q}_1 &= (\bar{s}\gamma^\mu P_L d)(\bar{u}\gamma_\mu P_L u), \\
\tilde{Q}_2 &= (\bar{s}_i\gamma^\mu P_L d_j)(\bar{u}_j\gamma_\mu P_L u_i), \\
\tilde{Q}_3 &= \sum_q (\bar{s}_i\gamma^\mu P_L q_j)(\bar{q}_j\gamma_\mu P_L d_i),
\end{aligned} \tag{2.67}$$

we can eliminate operators Q_4 , Q_9 and Q_{10} in such a way

$$\begin{aligned}
Q_4 &= \tilde{Q}_2 + \tilde{Q}_3 - Q_1, \\
Q_9 &= \frac{3}{2}\tilde{Q}_1 - \frac{1}{2}Q_3, \\
Q_{10} &= \frac{1}{2}(Q_1 - \tilde{Q}_3) + \tilde{Q}_2.
\end{aligned} \tag{2.68}$$

The remaining seven operators can then be recombined according to irreducible representations (irrep) of the chiral flavour-symmetry group $SU(3)_L \otimes SU(3)_R$. All the details of the decomposition can be found in the literature [23]. The chiral operator basis, which we will indicate with a primed, is thus given by

$$\begin{aligned}
(27, 1) \quad Q'_1 &= 3\tilde{Q}_1 + 2Q_2 - Q_3, \\
(8, 1) \quad Q'_2 &= \frac{1}{5}(2\tilde{Q}_1 - 2Q_2 + Q_3), \\
(8, 1) \quad Q'_3 &= \frac{1}{5}(-3\tilde{Q}_1 + 3Q_2 + Q_3), \\
(8, 1) \quad Q'_{5,6} &= Q_{5,6}, \\
(8, 8) \quad Q'_{7,8} &= Q_{7,8}
\end{aligned} \tag{2.69}$$

where (L, R) denotes the respective irrep of $SU(3)_L \otimes SU(3)_R$.

The conversion from the 7-operators chiral basis and the usual 10-operator basis is simply given by

$$Q_i = \sum_j T_{ij} Q'_j \tag{2.70}$$

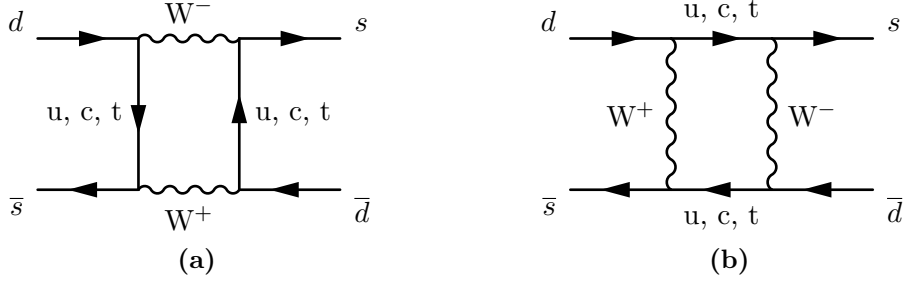


Figure 2.6. Box diagrams contributing to the $\Delta S = 2$ transitions.

where $1 \leq i \leq 10$ and $j \in \{1, 2, 3, 5, 6, 7, 8\}$ and the matrix T is given by

$$T = \begin{pmatrix} 1/5 & 1 & 0 & 0 & 0 & 0 & 0 \\ 1/5 & 0 & 1 & 0 & 0 & 0 & 0 \\ 0 & 3 & 2 & 0 & 0 & 0 & 0 \\ 0 & 2 & 3 & 0 & 0 & 0 & 0 \\ 0 & 0 & 0 & 1 & 0 & 0 & 0 \\ 0 & 0 & 0 & 0 & 1 & 0 & 0 \\ 0 & 0 & 0 & 0 & 0 & 1 & 0 \\ 0 & 0 & 0 & 0 & 0 & 0 & 1 \\ 3/10 & 0 & -1 & 0 & 0 & 0 & 0 \\ 3/10 & -1 & 0 & 0 & 0 & 0 & 0 \end{pmatrix} \quad (2.71)$$

2.2 Effective Hamiltonian for $\Delta S = 2$ Processes

Now we would like to do similar computations for $\Delta F = 2$ processes like the oscillations $K^0 \rightarrow \bar{K}^0$, which specifically are a $\Delta S = 2$ process since the underlying quark transition is given by $\bar{s}d \rightarrow \bar{d}s$.

Such FCNC process cannot arise at tree-level in the SM so we must consider one-loop contributions that, not considering the Goldstone boson exchange for now, are just the ones in fig. (2.6). Let us give now the computation for diagram (2.6a). Considering the external quark momenta to be zero, the amplitude can be easily found to be

$$\begin{aligned} i\mathcal{A}_a &= \int \frac{d^4\ell}{(2\pi)^4} \bar{u}^s \left(\frac{ig_2}{\sqrt{2}} \right) \gamma^\mu P_L V_{ujs}^* \frac{i(\ell - m_j)}{\ell^2 - m_j^2} \left(\frac{ig_2}{\sqrt{2}} \right) \gamma^\nu P_L V_{ujd} v^d \\ &\quad \bar{v}^s \left(\frac{ig_2}{\sqrt{2}} \right) \gamma_\nu P_L V_{uis}^* \frac{i(\ell - m_i)}{\ell^2 - m_i^2} \gamma_\mu P_L V_{uid} u^d \left(\frac{-i}{\ell^2 - M_W^2} \right)^2 \\ &= i \frac{g_2^4}{4} V_{uis}^* V_{uid} V_{ujs}^* V_{ujd} \int \frac{d^4\ell}{(2\pi)^4 (\ell^2 - M_W^2)^2} \\ &\quad \bar{u}^s \gamma^\mu P_L \frac{\ell - m_j}{\ell^2 - m_j^2} \gamma^\nu P_L v^d \bar{v}^s \gamma_\nu P_L \frac{\ell - m_i}{\ell^2 - m_i^2} \gamma_\mu P_L u^d, \end{aligned} \quad (2.72)$$

where m_i is the mass of the up-like quark u_i between the initial quarks and m_j the mass of the up-like quark u_j between the final quarks. The terms proportional to the mass in eq. (2.72) vanish because of the chiral projectors

$$m_j \bar{u}^s \gamma_\mu P_L \gamma_\nu P_L v^d = m_j \bar{u}^s \gamma_\mu \gamma_\nu \underbrace{P_R P_L}_{=0} v^d = 0, \quad (2.73)$$

therefore the amplitude simplifies to

$$i \frac{g_2^4}{4} V_{u_i s}^* V_{u_i d} V_{u_j s}^* V_{u_j d} (\bar{u}^s \gamma^\mu P_L \gamma^\alpha \gamma^\nu P_L v^d) (\bar{v}^s \gamma_\nu P_L \gamma^\beta \gamma_\mu P_L u^d) I_{\alpha\beta}^{ij}, \quad (2.74)$$

where

$$I_{\alpha\beta}^{ij} = \int \frac{d^4 \ell}{(2\pi)^4} \frac{\ell_\alpha \ell_\beta}{(\ell^2 - m_i^2)(\ell^2 - m_j^2)^2(\ell^2 - M_W^2)^2}. \quad (2.75)$$

Let us consider for now the tensor integral $I_{\alpha\beta}^{ij}$. We can simplify its structure by means of partial fractioning as follows

$$\begin{aligned} \frac{1}{(\ell^2 - m_i^2)(\ell^2 - m_j^2)^2} &= \frac{A}{\ell^2 - m_i^2} + \frac{B}{\ell^2 - m_j^2} \\ &= \frac{(A+B)\ell^2 - (Am_j^2 + Bm_i^2)}{(\ell^2 - m_i^2)(\ell^2 - m_j^2)^2}, \end{aligned} \quad (2.76)$$

which simply implies that

$$A = -B, \quad A = \frac{1}{m_i^2 - m_j^2} \quad (2.77)$$

therefore

$$\frac{1}{(\ell^2 - m_i^2)(\ell^2 - m_j^2)^2} = \frac{1}{m_i^2 - m_j^2} \left(\frac{1}{\ell^2 - m_i^2} - \frac{1}{\ell^2 - m_j^2} \right). \quad (2.78)$$

From this, we obtain that

$$I_{\alpha\beta}^{ij} = \frac{I_{\alpha\beta}^i - I_{\alpha\beta}^j}{m_i^2 - m_j^2}, \quad (2.79)$$

where

$$\begin{aligned} I_{\alpha\beta}^i &= \int \frac{d^4 \ell}{(2\pi)^4} \frac{\ell_\alpha \ell_\beta}{(\ell^2 - m - i^2)(\ell^2 - M_W^2)^2} \\ &= \frac{g_{\alpha\beta}}{4} \int \frac{d^4 \ell}{(2\pi)^4} \frac{(\ell^2 - m_i^2) + m_i^2}{(\ell^2 - M_W^2)^2(\ell^2 - m_i^2)} \\ &= \frac{g_{\alpha\beta}}{4} \left[m_i^2 \int \frac{d^4 \ell}{(2\pi)^4} \left(\frac{1}{(\ell^2 - M_W^2)^2(\ell^2 - m_i^2)} + \frac{1}{(\ell^2 - M_W^2)^2} \right) \right]. \end{aligned} \quad (2.80)$$

The second term which does not depend on the quark mass cancels in the difference in eq. (2.79), therefore we can neglect it. While the first term becomes

$$\begin{aligned} \int \frac{d^4 \ell}{(2\pi)^d} \frac{1}{(\ell^2 - M_W^2)^2(\ell^2 - m_i^2)} &= 2 \int_0^1 dx \int \frac{d^4 \ell}{(2\pi)^d} \frac{x}{[(\ell^2 - M_W^2)x + (\ell^2 - m_i^2)(1-x)]^3} \\ &= 2 \int_0^1 dx \int \frac{d^4 \ell}{(2\pi)^4} \frac{x}{[\ell^2 - (xM_W^2 + (1-x)m_i^2)]^3}. \end{aligned} \quad (2.81)$$

The integral in the loop momentum is convergent

$$\int \frac{d^4 \ell}{(2\pi)^4} \frac{x}{[\ell^2 - (xM_W^2 + (1-x)m_i^2)]^3} = -\frac{i}{16\pi^2} \frac{1}{2} \frac{1}{xM_W^2 + (1-x)m_i^2} \quad (2.82)$$

as can be easily seen by analytically continuing to d -dimensions and then taking the limit $d \rightarrow 4$. Hence the integral of eq. (2.81) becomes

$$\begin{aligned}
&= -\frac{i}{16\pi^2} \int_0^1 dx \frac{x}{xM_W^2 + (1-x)m_i^2} \\
&= -\frac{i}{16\pi^2 M_W^2} \int_0^1 \frac{x}{x + x_i(1-x)} \\
&= -\frac{i}{16\pi^2 M_W^2} \int_0^1 dx \frac{x}{x_i + x(1-x_i)} \\
&= -\frac{i}{16\pi^2 M_W^2} \int_0^1 \frac{dx}{(1-x_i)} \frac{(1-x_i)x + x_i - x_i}{x_i + x(1-x_i)} \\
&= -\frac{i}{16\pi^2 M_W^2} \left(\frac{-x_i}{1-x_i} \int_0^1 dx \frac{1}{(1-x_i)x + x_i} + \frac{1}{1-x_i} \right) \\
&= -\frac{i}{16\pi^2 M_W^2} \left(\frac{1}{1-x_i} + \frac{x_i \log x_i}{(1-x_i)^2} \right),
\end{aligned} \tag{2.83}$$

where $x_i = m_i^2/M_W^2$. Thus, up to terms that do not depend on m_i we get

$$\begin{aligned}
I_{\alpha\beta}^i &= -\frac{g_{\alpha\beta}}{4} \frac{i}{16\pi^2} \frac{m_i^2}{M_W^2} \left(\frac{1}{1-x_i} + \frac{x_i \log x_i}{(1-x_i)^2} \right) \\
&= -\frac{g_{\alpha\beta}}{4} \frac{i}{16\pi^2} J(x_i),
\end{aligned} \tag{2.84}$$

where

$$J(x_i) = \frac{x_i}{1-x_i} + \frac{x_i^2 \log x_i}{(1-x_i)^2}. \tag{2.85}$$

Therefore

$$I_{\alpha\beta}^{ij} = -\frac{g_{\alpha\beta}}{4M_W^2} \frac{i}{16\pi^2} A(x_i, x_j), \tag{2.86}$$

where

$$A(x_i, x_j) = \frac{J(x_i) - J(x_j)}{x_i - x_j}. \tag{2.87}$$

This is our first, actually computed, Inami-Lim function [22] which encodes the loop information of the diagram.

We now turn our attention to the Dirac structure of eq. (2.74)

$$\bar{u}^d \gamma^\mu P_L \gamma^\alpha \gamma^\nu P_L v^d \bar{v}^s \gamma_\nu P_L \gamma^\beta \gamma_\mu P_L u^d. \tag{2.88}$$

By using the usual projector rules and Clifford algebra, together with the $g_{\alpha\beta}$ from the integral, we can highlight the usual structure

$$\bar{u}^s \gamma^\mu \gamma^\alpha \gamma^\nu \left(P_L v^d \bar{v}^s P_R \right) \gamma_\nu \gamma_\alpha \gamma_\mu u^d \tag{2.89}$$

and by using the Fierz identities

$$(P_L v^d \bar{v}^s P_R)_{\alpha\beta} = -\frac{1}{2} \bar{v}^s \gamma^\rho P_L v^d (\gamma_\rho P_R)_{\alpha\beta} \tag{2.90}$$

we obtain

$$-\frac{1}{2}\bar{v}^s\gamma^\rho P_L v^d \bar{u}^s\gamma^\mu\gamma^\alpha\gamma^\nu\gamma_\rho P_R\gamma_\nu\gamma_\alpha\gamma_\mu u^d, \quad (2.91)$$

then by jumping the P_R over the gamma matrices

$$-\frac{1}{2}\bar{v}^s\gamma^\rho P_L v^d \bar{u}^s\gamma^\mu\gamma^\alpha\gamma^\nu\gamma_\rho\gamma_\nu\gamma_\alpha\gamma_\mu P_L u^d = 4\bar{v}^s\gamma^\rho P_L v^d \bar{u}^s\gamma_\rho P_L u^d, \quad (2.92)$$

where we used the usual relation $\gamma^\alpha\gamma^\mu\gamma_\alpha = -2\gamma^\mu$ four times.

Putting everything together we obtain the amplitude for the diagram (2.6a) as

$$\begin{aligned} i\mathcal{A}_a &= -\frac{i}{16\pi^2} \frac{4g_2^4}{16M_W^2} \sum_{i,j=u,c,t} V_{is}^* V_{id} V_{js}^* V_{jd} A(x_i, x_j) \bar{v}^s\gamma^\mu P_L v^d \bar{u}^s\gamma_\mu P_L u^d \\ &= -\frac{iG_F^2 M_W^2}{2\pi^2} \sum_{i,j=u,c,t} \lambda_{sd}^i \lambda_{sd}^j A(x_i, x_j) \bar{v}^s\gamma^\mu P_L v^d \bar{u}^s\gamma_\mu P_L u^d, \end{aligned} \quad (2.93)$$

where $\lambda_{sd}^i = V_{is}^* V_{id}$.

The computation of diagram (2.6b) goes along the same lines as for diagram (2.6a), where we just need to exchange an incoming \bar{s} to an outgoing s and vice-versa. If we put the spinors in the amplitude

$$\begin{aligned} i\mathcal{A}_a &= -\frac{iG_F^2 M_W^2}{2\pi^2} \sum_{i,j=u,c,t} \lambda_{sd}^i \lambda_{sd}^j A(x_i, x_j) \bar{v}_s\gamma^\mu P_L v_d \bar{u}_s\gamma_\mu P_L u_d \\ i\mathcal{A}_b &= \frac{iG_F^2 M_W^2}{2\pi^2} \sum_{i,j=u,c,t} \lambda_{sd}^i \lambda_{sd}^j A(x_i, x_j) \bar{u}_s\gamma^\mu P_L u_d \bar{v}_s\gamma_\mu P_L v_d. \end{aligned} \quad (2.94)$$

Both these amplitudes can be written as the matrix elements of the same local operator, which lets us write the effective $\Delta S = 2$ Hamiltonian as

$$\mathcal{H}_{\text{eff}}^{\Delta S=2} = C \bar{s}\gamma^\mu P_L d \bar{s}\gamma_\mu P_L d \quad (2.95)$$

where C is a Wilson coefficient. This effective Hamiltonian generates the following amplitude

$$-iC \langle \bar{d}s | \bar{s}\gamma^\mu P_L d \bar{s}\gamma_\mu P_L d | \bar{s}d \rangle = -2iC (\bar{u}_s\gamma^\mu P_L v_d \bar{v}_s\gamma_\mu P_L u_d - \bar{u}_s\gamma^\mu P_L u_d \bar{v}_s\gamma_\mu P_L v_d). \quad (2.96)$$

By matching with the full amplitude, we get that

$$C^{a+b} = \frac{G_F^2 M_W^2}{4\pi^2} \sum_{i,j=u,c,t} \lambda_{sd}^i \lambda_{sd}^j A(x_i, x_j). \quad (2.97)$$

There remains to evaluate also the box diagrams with the Goldstone boson exchange. We do not delve into the details of the calculation but, once evaluated, the same matching procedure as before can be done, obtaining three more Wilson coefficients, two coming from a single Goldstone exchange and one from the double Goldstone exchange, which are given by

$$\begin{aligned} C_2 = C_3 &= -\frac{G_F^2 M_W^2}{4\pi^2} \sum_{i,j=u,c,t} \lambda_{sd}^i \lambda_{sd}^j A'(x_i, x_j) x_i x_j \\ C_4 &= \frac{G_F^2 M_W^2}{8\pi^2} \sum_{i,j=u,c,t} \lambda_{sd}^i \lambda_{sd}^j A(x_i, x_j) x_i x_j, \end{aligned} \quad (2.98)$$

where

$$A'(x_i, x_j) = \frac{J'(x_i) - J'(x_j)}{x_i - x_j}, \quad J'(x) = \frac{1}{1-x} + \frac{x \log x}{(1-x)^2}. \quad (2.99)$$

In the end, by putting everything together, we get

$$C = \frac{G_F^2 M_W^2}{4\pi^2} \sum_{i,j=u,c,t} \lambda_{sd}^i \lambda_{sd}^j \bar{A}(x_i, x_j), \quad (2.100)$$

where

$$\bar{A}(x_i, x_j) = A(x_i, x_j) - x_i x_j A'(x_i, x_j) + \frac{1}{4} x_i x_j A(x_i, x_j). \quad (2.101)$$

By using the CKM unitarity, we can finally write down the full $\Delta S = 2$ effective Hamiltonian as

$$\mathcal{H}_{\text{eff}}^{\Delta S=2} = \frac{G_F^2 M_W^2}{4\pi^2} \left[(\lambda_{sd}^t)^2 S_0(x_t) + (\lambda_{sd}^c)^2 S_0(x_c) + 2\lambda_{sd}^t \lambda_{sd}^c S_0(x_c, x_t) \right] \bar{s} \gamma^\mu P_L d \bar{s} \gamma_\mu P_L d, \quad (2.102)$$

where

$$\begin{aligned} S_0(x) &= \bar{A}(x, x) + \bar{A}(x_u, x_u) - 2\bar{A}(x_u, x), \\ S_0(x, y) &= \bar{A}(x, y) + \bar{A}(x_u, x_u) - \bar{A}(x_u, x) - \bar{A}(x_u, y). \end{aligned} \quad (2.103)$$

All the calculations we have done so far are in the limit of zero external quark momenta. This is a good limit if there is no explicit dependence on the quark momenta. This turns out to be a good approximation but with some additional details that we will not discuss here [9, 30].

What we might want now to do, is to include LO QCD corrections in the same fashion as done for the $\Delta S = 1$ effective Hamiltonian. What changes is that the inclusion of loop corrections, does not add a new operator with a different color structure to the basis since, by means of Fierz identities, we can go back to the original color structure.

This leads to the following anomalous dimension

$$\gamma^{(0)} = 6 \frac{N-1}{N}. \quad (2.104)$$

A complete treatment of the NLO QCD corrections is beyond the scope of this thesis but can be found in the literature [5, 19, 20, 21]. These corrections are usually parametrized by three factors η_1, η_2 and η_3 . The effective Hamiltonian is usually written in the following form

$$\begin{aligned} \mathcal{H}_{\text{eff}}^{\Delta S=2} &= \frac{G_F^2 M_W^2}{4\pi^2} \left[(\lambda_{sd}^t)^2 \eta_2 S_0(x_t) + (\lambda_{sd}^c)^2 \eta_1 S_0(x_c) \right. \\ &\quad \left. + 2\lambda_{sd}^t \lambda_{sd}^c \eta_3 S_0(x_c, x_t) \right] \bar{s} \gamma^\mu P_L d \bar{s} \gamma_\mu P_L d, \end{aligned} \quad (2.105)$$

where $\eta_i = 1 + \mathcal{O}(\alpha_s)$.

Bibliography

- [1] ABBOTT, R. ET AL. Direct CP violation and the $\Delta I = 1/2$ rule in $K \rightarrow \pi\pi$ decay from the standard model. *Phys. Rev. D*, **102** (2020), 054509. [arXiv:2004.09440](#), [doi:10.1103/PhysRevD.102.054509](#).
- [2] ALTARELLI, G. AND MAIANI, L. Octet Enhancement of Nonleptonic Weak Interactions in Asymptotically Free Gauge Theories. *Phys. Lett. B*, **52** (1974), 351. [doi:10.1016/0370-2693\(74\)90060-4](#).
- [3] BERTOLINI, S., EEG, J. O., AND FABBRICHESI, M. Studying epsilon-prime / epsilon in the chiral quark model: gamma(5) scheme independence and NLO hadronic matrix elements. *Nucl. Phys. B*, **449** (1995), 197. [arXiv:hep-ph/9409437](#), [doi:10.1016/0550-3213\(95\)00274-V](#).
- [4] BUCHALLA, G., BURAS, A. J., AND LAUTENBACHER, M. E. Weak decays beyond leading logarithms. *Rev. Mod. Phys.*, **68** (1996), 1125. [arXiv:hep-ph/9512380](#), [doi:10.1103/RevModPhys.68.1125](#).
- [5] BURAS, A. J. Weak Hamiltonian, CP violation and rare decays. In *Les Houches Summer School in Theoretical Physics, Session 68: Probing the Standard Model of Particle Interactions* (1998). [arXiv:hep-ph/9806471](#).
- [6] BURAS, A. J., GAMBINO, P., AND HAISCH, U. A. Electroweak penguin contributions to nonleptonic Delta F = 1 decays at NNLO. *Nucl. Phys. B*, **570** (2000), 117. [arXiv:hep-ph/9911250](#), [doi:10.1016/S0550-3213\(99\)00810-X](#).
- [7] BURAS, A. J., JAMIN, M., AND LAUTENBACHER, M. E. Two loop anomalous dimension matrix for Delta S = 1 weak nonleptonic decays. 2. O(alpha-alpha-s). *Nucl. Phys. B*, **400** (1993), 75. [arXiv:hep-ph/9211321](#), [doi:10.1016/0550-3213\(93\)90398-9](#).
- [8] BURAS, A. J., JAMIN, M., LAUTENBACHER, M. E., AND WEISZ, P. H. Effective Hamiltonians for $\Delta S = 1$ and $\Delta B = 1$ nonleptonic decays beyond the leading logarithmic approximation. *Nucl. Phys. B*, **370** (1992), 69. [Addendum: *Nucl.Phys.B* 375, 501 (1992)]. [doi:10.1016/0550-3213\(92\)90345-C](#).
- [9] CATA, O. AND PERIS, S. Long distance dimension eight operators in B(K). *JHEP*, **03** (2003), 060. [arXiv:hep-ph/0303162](#), [doi:10.1088/1126-6708/2003/03/060](#).

- [10] CIUCHINI, M., FRANCO, E., MARTINELLI, G., AND REINA, L. ϵ'/ϵ at the Next-to-leading order in QCD and QED. *Phys. Lett. B*, **301** (1993), 263. [arXiv:hep-ph/9212203](#), [doi:10.1016/0370-2693\(93\)90699-1](#).
- [11] CIUCHINI, M., FRANCO, E., MARTINELLI, G., AND REINA, L. The Delta $S = 1$ effective Hamiltonian including next-to-leading order QCD and QED corrections. *Nucl. Phys. B*, **415** (1994), 403. [arXiv:hep-ph/9304257](#), [doi:10.1016/0550-3213\(94\)90118-X](#).
- [12] CONSTANTINOU, M., COSTA, M., FREZZOTTI, R., LUBICZ, V., MARTINELLI, G., MELONI, D., PANAGOPOULOS, H., AND SIMULA, S. $K \rightarrow \pi$ matrix elements of the chromomagnetic operator on the lattice. *Phys. Rev. D*, **97** (2018), 074501. [arXiv:1712.09824](#), [doi:10.1103/PhysRevD.97.074501](#).
- [13] FERMI, E. An attempt of a theory of beta radiation. 1. *Z. Phys.*, **88** (1934), 161. [doi:10.1007/BF01351864](#).
- [14] FIERZ, M. Zur fermischen theorie des β -zerfalls. *Zeitschrift für Physik*, **104** (1937), 553. Available from: <https://doi.org/10.1007/BF01330070>, [doi:10.1007/BF01330070](#).
- [15] GAILLARD, M. K. AND LEE, B. W. $\Delta I = 1/2$ Rule for Nonleptonic Decays in Asymptotically Free Field Theories. *Phys. Rev. Lett.*, **33** (1974), 108. [doi:10.1103/PhysRevLett.33.108](#).
- [16] GILMAN, F. J. AND WISE, M. B. Effective Hamiltonian for Delta $s = 1$ Weak Nonleptonic Decays in the Six Quark Model. *Phys. Rev. D*, **20** (1979), 2392. [doi:10.1103/PhysRevD.20.2392](#).
- [17] GORBAHN, M. AND HAISCH, U. Effective Hamiltonian for non-leptonic $|\Delta F| = 1$ decays at NNLO in QCD. *Nucl. Phys. B*, **713** (2005), 291. [arXiv:hep-ph/0411071](#), [doi:10.1016/j.nuclphysb.2005.01.047](#).
- [18] GUBERINA, B. AND PECCEI, R. D. Quantum Chromodynamic Effects and CP Violation in the Kobayashi-Maskawa Model. *Nucl. Phys. B*, **163** (1980), 289. [doi:10.1016/0550-3213\(80\)90404-6](#).
- [19] HERRLICH, S. AND NIERSTE, U. Enhancement of the $K(L) - K(S)$ mass difference by short distance QCD corrections beyond leading logarithms. *Nucl. Phys. B*, **419** (1994), 292. [arXiv:hep-ph/9310311](#), [doi:10.1016/0550-3213\(94\)90044-2](#).
- [20] HERRLICH, S. AND NIERSTE, U. Indirect CP violation in the neutral kaon system beyond leading logarithms. *Phys. Rev. D*, **52** (1995), 6505. [arXiv:hep-ph/9507262](#), [doi:10.1103/PhysRevD.52.6505](#).
- [21] HERRLICH, S. AND NIERSTE, U. The Complete $|\Delta S| = 2$ - Hamiltonian in the next-to-leading order. *Nucl. Phys. B*, **476** (1996), 27. [arXiv:hep-ph/9604330](#), [doi:10.1016/0550-3213\(96\)00324-0](#).

- [22] INAMI, T. AND LIM, C. S. Effects of Superheavy Quarks and Leptons in Low-Energy Weak Processes $K_L \rightarrow \mu\bar{\mu}$, $K^+ \rightarrow \pi^+\nu\bar{\nu}$ and $K^0 - \bar{K}^0$. *Prog. Theor. Phys.*, **65** (1981), 297. [Erratum: *Prog.Theor.Phys.* 65, 1772 (1981)]. [doi:10.1143/PTP.65.297](https://doi.org/10.1143/PTP.65.297).
- [23] LEHNER, C. AND STURM, C. Matching factors for Delta S=1 four-quark operators in RI/SMOM schemes. *Phys. Rev. D*, **84** (2011), 014001. [arXiv:1104.4948](https://arxiv.org/abs/1104.4948), [doi:10.1103/PhysRevD.84.014001](https://doi.org/10.1103/PhysRevD.84.014001).
- [24] MANOHAR, A. V. Effective field theories. *Lect. Notes Phys.*, **479** (1997), 311. [arXiv:hep-ph/9606222](https://arxiv.org/abs/hep-ph/9606222), [doi:10.1007/BFb0104294](https://doi.org/10.1007/BFb0104294).
- [25] MARTINELLI, G., PITTORI, C., SACHRAJDA, C. T., TESTA, M., AND VLADIKAS, A. A General method for nonperturbative renormalization of lattice operators. *Nucl. Phys. B*, **445** (1995), 81. [arXiv:hep-lat/9411010](https://arxiv.org/abs/hep-lat/9411010), [doi:10.1016/0550-3213\(95\)00126-D](https://doi.org/10.1016/0550-3213(95)00126-D).
- [26] NEUBERT, M. Renormalization Theory and Effective Field Theories. (2019). [arXiv:1901.06573](https://arxiv.org/abs/1901.06573), [doi:10.1093/oso/9780198855743.003.0001](https://doi.org/10.1093/oso/9780198855743.003.0001).
- [27] PICH, A. Chiral perturbation theory. *Rept. Prog. Phys.*, **58** (1995), 563. [arXiv:hep-ph/9502366](https://arxiv.org/abs/hep-ph/9502366), [doi:10.1088/0034-4885/58/6/001](https://doi.org/10.1088/0034-4885/58/6/001).
- [28] POLCHINSKI, J. Effective field theory and the Fermi surface. In *Theoretical Advanced Study Institute (TASI 92): From Black Holes and Strings to Particles* (1992). [arXiv:hep-th/9210046](https://arxiv.org/abs/hep-th/9210046).
- [29] SHIFMAN, M. A. Foreword to ITEP lectures in particle physics (1995). [arXiv:hep-ph/9510397](https://arxiv.org/abs/hep-ph/9510397).
- [30] SILVESTRINI, L. Effective theories for quark flavour physics (2021). [arXiv:1905.00798](https://arxiv.org/abs/1905.00798).
- [31] 'T HOOFT, G. Large N. In *The Phenomenology of Large N(c) QCD* (2002). [arXiv:hep-th/0204069](https://arxiv.org/abs/hep-th/0204069), [doi:10.1142/9789812776914_0001](https://doi.org/10.1142/9789812776914_0001).
- [32] VAINSHTEIN, A. I., ZAKHAROV, V. I., AND SHIFMAN, M. A. A Possible mechanism for the Delta T = 1/2 rule in nonleptonic decays of strange particles. *JETP Lett.*, **22** (1975), 55.
- [33] VAĬNSHTEĬN, A. I., ZAKHAROV, V. I., AND SHIFMAN, M. A. A possible mechanism for the $\Delta T = 1/2$ rule in nonleptonic decays of strange particles. *Soviet Journal of Experimental and Theoretical Physics Letters*, **22** (1975), 55.
- [34] VAĬNSHTEĬN, A. I., ZAKHAROV, V. I., AND SHIFMAN, M. A. A possible mechanism for the $\Delta T = 1/2$ rule in nonleptonic decays of strange particles. *ZhETF Pisma Redaktsiiu*, **22** (1975), 123.
- [35] WILSON, K. G. AND ZIMMERMANN, W. Operator product expansions and composite field operators in the general framework of quantum field theory. *Commun. Math. Phys.*, **24** (1972), 87. [doi:10.1007/BF01878448](https://doi.org/10.1007/BF01878448).